



PERGAMON

International Journal of Solids and Structures 40 (2003) 2563–2588

INTERNATIONAL JOURNAL OF
SOLIDS and
STRUCTURES

www.elsevier.com/locate/ijsolstr

On a formulation for a multiscale atomistic-continuum homogenization method

Peter W. Chung ^{*}, Raju R. Namburu

*Computational and Information Sciences Directorate, US Army Research Laboratory,
AMSRL-CI-HC, Aberdeen Proving Ground, MD 21005-5067, USA*

Received 7 November 2001

Abstract

The homogenization method is used as a framework for developing a multiscale system of equations involving atoms at zero temperature at the small scale and continuum mechanics at the very large scale. The Tersoff–Brenner Type II potential [Physical Review Letters 61(25) (1988) 2879; Physical Review B 42 (15) (1990) 9458] is employed to model the atomic interactions while hyperelasticity governs the continuum. A quasistatic assumption is used together with the Cauchy–Born approximation to enforce the gross deformation of the continuum on the positions of the atoms. The two-scale homogenization method establishes coupled self-consistent variational equations in which the information at the atomistic scale, formulated in terms of the Lagrangian stiffness tensor, concurrently feeds the material information to the continuum equations. Analytical results for a one dimensional molecular wire and numerical experiments for a two dimensional graphene sheet demonstrate the method and its applicability.

Published by Elsevier Science Ltd.

Keywords: Homogenization; Atomic-level; Multiscale; Graphene; Lattice statics; Finite element method

1. Introduction

A large amount of research interest has focused on the multiscale problem involving atoms and continua. It is widely accepted that many effects on the continuum germinate at the atomic level. Events such as fracture, fatigue, and inelastic material response can be traced back to phenomena in the atomic structure. Moreover, fabrication of nanoscale devices in mass quantities will likely come from nanopatterning techniques (e.g., see (Rosa et al., 2000)). Creating patterns at the nanometer scale will likely involve unforeseen effects when coupled to mechanical loads. Therefore, a computational mechanics method is necessary that can couple disparate scales—one scale in which the boundary conditions are applied and the other in which atoms reside.

Methodologies for linking a continuum to an atomistic domain can be found in the literature as early as 1971 (Sinclair, 1971). Finite element methods were later employed by Mullins and Dokainish (1982) using a

^{*} Corresponding author. Tel.: +1-410-278-6027; fax: +1-410-278-4983.

E-mail address: pchung@arl.army.mil (P.W. Chung).

numerically decoupled domain approach with spatially overlapping atomistic and continuum regions. A review of some of these methods can be found by Cleri et al. (1998). Among these early analytic and computational studies, frequent issues regarding the treatment of the interface arose which were primarily handled through creative use of kinematic constraints.

More recently Tadmor et al. (1996) developed a finite element-based formulation, the so-called quasi-continuum method. Similar efforts were made through the so-called handshaking or coupling-of-length-scales (CLS) method by Broughton et al. (1999) by increasing the atomic resolution to account for electron degrees of freedom via the tight-binding (TB) method. The dynamic problem was studied with a generalized scaling approach in coarse-grained molecular dynamics (CGMD) by Rudd and Broughton (2000) to better handle the propagation of waves through the atomistic-FE interface and the FE far field.

Multiscale methods such as these have traditionally been limited mainly to localized regions of interest. For example, the applications to which these methods have been applied involve small sets of dislocations and cracks and limited analyses of their mutual interactions. The localized regions on which these simulations are run typically span, at most, tens of microns because of the bottleneck imposed by a direct interface between the continuum region and atomistic region. To ensure compatibility, kinematic constraints are used to tie together the equations and disparate length scales across this interface. Driving the resolution of the discretized continuum finite elements down to the atom scale intrinsically restricts the size of the continuum and leads to smaller overall dimensions of the problem. This can only be overcome by larger use of computer resources when dealing with problems with larger dimensions.

The asymptotic expansion homogenization method has been widely studied by applied mathematicians for many years. Numerous texts on the basic theory can be found in the literature, for instance, by Bensoussan et al. (1978), Sanchez-Palencia (1980), and Bakhvalov and Panasenko (1989). Yet, despite the prolific research in the field, no attempts have been documented for extending the technique to atoms.

Homogenization may be particularly suited for nanopatterned systems because of its use of periodicity and asymptotics in the assumptions; perhaps even more so than traditional homogenization applications, such as composites. This is because in most cases the ratio of scales in atomistic-continuum problems better represents the asymptotic assumption in homogenization than other types of multiscale problems. Furthermore, the periodic nature of nanopatterned systems is more apt at realistically adhering to the periodic assumption than unit cell models of composite material inclusions.

In this paper, a computational framework for homogenization of the atomistic problem is presented. Using two concurrent domains, one for the macroscale continuum domain and one for the periodic atomic scale domain, self-consistent sets of equations are derived. Atoms in arbitrary configurations and structures of unlimited size are permitted. Through the asymptotic expansion homogenization technique, a set of hierarchical equations are derived based on hyperelasticity. At the local level, the atomistic equations are used under the assumption of the harmonic approximation to generate the effective properties needed to solve the effective global level equations. The Cauchy–Born rule (Ericksen, 1984) is applied to the atoms to enforce the gross deformation of the continuum on the atoms. This circumvents the need to apply kinematic constraints by making use of the averaging features of homogenization.

The contents of this paper are as follows. In Section 2, the conventional continuum equations are shown, eventually leading to a variational form based on the principle of virtual work. Then, in Section 3, the multiscale equations are developed, resulting in two sets of equations which govern the local and global length scales. By introducing the atomistic potential in Sections 4 and 5, the details of the atomistic formulations are presented and cast in a variational form for use in the multiscale homogenization method. In Section 6, the derivatives of the atomistic energy potential needed to complete the derivation of the method are provided in a general form. In Section 7, 1-D and 2-D demonstrative examples are shown. Closing remarks are discussed in Section 8. Additional details of the analytical derivatives of the Tersoff–Brenner Type II potential are presented in Appendix A.

2. Continuum formulations

This section describes the kinematics, stress definitions, and linear momentum conservation laws needed to develop the homogenization method from atomistic principles.

2.1. Kinematics

Consider an open set V in \mathfrak{R}^3 that deforms to the configuration v in \mathfrak{R}^3 . Points in V are denoted $\mathbf{X} = (X_1, X_2, X_3) \in V$ and are called material points, while points in v are denoted $\mathbf{x} = (x_1, x_2, x_3) \in v$ and are called spatial points. The deformation is a one-to-one mapping through ϕ so that $x = \phi(X)$. The deformation gradient is defined by

$$\mathbf{F} = \frac{\partial \phi}{\partial \mathbf{X}} = \frac{\partial \mathbf{x}}{\partial \mathbf{X}} = \nabla_0 \mathbf{x} \quad \text{and} \quad F_{ij} = \frac{\partial \phi_i}{\partial X_j} = \frac{\partial x_i}{\partial X_j}, \quad (1)$$

where ∇_0 signifies the gradient taken with respect to the material frame. The determinant of F is termed the Jacobian and is defined by $J = \det \mathbf{F}$. The right Cauchy-Green strain tensor is defined by

$$\mathbf{C} = \mathbf{F}^T \mathbf{F}, \quad (2)$$

and the Green strain tensor is defined by

$$\mathbf{E} = \frac{1}{2}(\mathbf{C} - \mathbf{I}). \quad (3)$$

2.2. Stress and equilibrium

The material representation for the conservation of linear momentum is defined by

$$\nabla_0 \cdot \mathbf{P} + \mathbf{f}_0 = 0, \quad (4)$$

where \mathbf{P} is the first Piola–Kirchoff stress tensor and \mathbf{f}_0 is the body force per unit of undeformed volume. In rate form, it is given by

$$\nabla_0 \cdot \dot{\mathbf{P}} + \dot{\mathbf{f}}_0 = 0. \quad (5)$$

Using the principle of virtual work, Eq. (5) can be rewritten as

$$\int_V (\nabla_0 \cdot \dot{\mathbf{P}}) \delta \mathbf{u} dV + \int_V \dot{\mathbf{f}}_0 \cdot \delta \mathbf{u} dV = 0, \quad \forall \delta \mathbf{u}, \quad (6)$$

where $\delta \mathbf{u}$ is the virtual displacement. Then, using the definition for traction with respect to the undeformed body, Eq. (6) can be rewritten as

$$\int_V \dot{\mathbf{P}} : \nabla_0 \delta \mathbf{u} dV = \int_{\partial V} \dot{\mathbf{t}}_0 \cdot \delta \mathbf{u} dA + \int_V \dot{\mathbf{f}}_0 \cdot \delta \mathbf{u} dV. \quad (7)$$

We invoke the notion of hyperelasticity by assuming that the atomistic potential, \mathcal{W} , which is a function of the atom positions, can be expressed in terms of strain. This assumes that the strain energy density (or the free energy at zero temperature) is equivalent to the atomistic energy potential. Following classical continuum mechanics, one can then define the first Piola–Kirchoff stress as

$$\mathbf{P} = \frac{\partial \mathcal{W}}{\partial \mathbf{F}} \quad \text{and} \quad P_{ij} = \frac{\partial \mathcal{W}}{\partial F_{ij}}, \quad (8)$$

and the first Lagrangian elasticity tensor (Marsden and Hughes, 1983) as

$$\mathcal{C} = \frac{\partial^2 \mathcal{W}}{\partial \mathbf{F} \partial \mathbf{F}} = \frac{\partial \mathbf{P}}{\partial \mathbf{F}} \quad \text{and} \quad \mathcal{C}_{ijkl} = \frac{\partial^2 \mathcal{W}}{\partial F_{ij} \partial F_{kl}} = \frac{\partial P_{ij}}{\partial F_{kl}}. \quad (9)$$

A relationship is needed between stress and strain. From Eq. (9), one can see that in hyperelastic materials, \mathbf{P} is related to \mathbf{F} through

$$\dot{\mathbf{P}} = \mathcal{C} \dot{\mathbf{F}} \quad \text{and} \quad \dot{P}_{ij} = \mathcal{C}_{ijkl} \dot{F}_{kl}, \quad (10)$$

where

$$\dot{\mathbf{F}} = \partial \dot{\mathbf{u}} / \partial \mathbf{X} = \partial \mathbf{v} / \partial \mathbf{X}, \quad (11)$$

and where $\dot{\mathbf{u}} = \mathbf{v}$ denotes the velocity.

Substituting Eq. (10) into (7) and using (11) yields

$$\int_V \mathcal{C} : (\nabla_0 \delta \mathbf{u} \otimes \nabla_0 \mathbf{v}) dV = \int_{\partial V} \mathbf{t}_0 \cdot \delta \mathbf{u} dA + \int_V \mathbf{f}_0 \cdot \delta \mathbf{u} dV, \quad \forall \delta \mathbf{u}, \quad (12)$$

and the equivalent indicial form,

$$\int_V \mathcal{C}_{ijkl} \frac{\partial \delta u_i}{\partial X_j} \frac{\partial v_k}{\partial X_l} dV = \int_{\partial V} \mathbf{t}_{0i} \delta u_i dA + \int_V f_{0i} \delta u_i dV. \quad (13)$$

This is the virtual work equation associated with hyperelasticity. The two-scale approach is described next. It is devised so that traditional finite element continuum equations can be solved in the coarse scale and atomistic equations can be solved in the fine scale.

3. Homogenization

The homogenization framework enables the *weak* coupling of the continuum to the atoms. By taking the limit of the time-independent asymptotic expansion parameter $\varepsilon \rightarrow 0$, we exploit the weak convergence properties of the scheme in order to decouple the length scales. At the fine scale, the domain contains only atoms with periodic conditions prescribed on the boundary, and all atom displacements are measured relative to a fixed point in the local frame of reference. From classical examples of continuum mechanics of composite materials (Mura, 1987) this enables the method to account for mutual interactions of periodically spaced heterogeneities or, in this case, periodic lattice defects. It should be noted that for this formulation, any general periodic arrangement of atoms may be treated such as quantum dots or epitaxial systems (Tang and Torres, 1996), as long as the interest is in mechanical and deformation coupling of the atoms with macroscopic scales.

The homogenization method is based on the assumption that two scales exist—a coarse scale and a fine scale. Coordinates in the coarse material scale are $\mathbf{X} = (X_1, X_2, X_3)$, and those in the fine material scale are $\mathbf{Y} = (Y_1, Y_2, Y_3)$. Likewise, the spatial coordinates are the lowercase analogues. The two scales are related by the scale parameter

$$\mathbf{Y} = \frac{\mathbf{X}}{\varepsilon}. \quad (14)$$

Therefore, we assume that the ratio of scales remains the same before and after deformation. The aim is to obtain two sets of coupled equations. The asymptotic series assumption decomposes the displacements as

$$\mathbf{u}(\mathbf{X}) = \mathbf{u}^{[0]}(\mathbf{X}) + \mathbf{u}^{[1]}(\mathbf{X}) \quad (15)$$

$$= \mathbf{u}^{[0]}(\mathbf{X}) + \varepsilon \mathbf{u}^{[1]}(\mathbf{Y}), \quad (16)$$

where $\mathbf{u}^{[0]}$ represents the displacement at the coarse scale and $\mathbf{u}^{[1]}$ represents the perturbed displacements due to inhomogeneity at the fine scale. Square brackets denote the order of the term in the asymptotic series. The actual physical representation of the total displacement at the fine scale is given by Takano et al. (2000) as

$$\begin{aligned} \frac{1}{\varepsilon} \mathbf{u}(\mathbf{X}) &= \mathbf{u}^{\text{micro}}(\mathbf{Y}) \\ &= \mathbf{F}(\mathbf{u}^{[0]}(\mathbf{X})) \mathbf{Y} + \mathbf{u}^{[1]}(\mathbf{Y}). \end{aligned} \quad (17)$$

The variable \mathbf{X} in Eq. (17) is a fixed value with respect to \mathbf{Y} . That is, the deformation gradient of a point in the coarse scale gets mapped onto a fine scale grid. This point is typically a quadrature point in a finite element sense.

The time derivatives are analogous to Eqs. (16) and (17). They are given as

$$\begin{aligned} \dot{\mathbf{u}}(\mathbf{X}) &= \mathbf{v}(\mathbf{X}) \\ &= \mathbf{v}^{[0]}(\mathbf{X}) + \varepsilon \mathbf{v}^{[1]}(\mathbf{Y}), \end{aligned} \quad (18)$$

$$\begin{aligned} \dot{\mathbf{u}}^{\text{micro}}(\mathbf{Y}) &= \mathbf{v}^{\text{micro}}(\mathbf{X}) \\ &= \mathbf{F}(\mathbf{v}^{[0]}(\mathbf{X})) \mathbf{Y} + \mathbf{v}^{[1]}(\mathbf{Y}). \end{aligned} \quad (19)$$

Substituting Eqs. (16) and (18) into Eq. (13) yields

$$\begin{aligned} \int_V \mathcal{C} :: & [\nabla_X (\delta \mathbf{u}^{[0]}(\mathbf{X}) + \varepsilon \delta \mathbf{u}^{[1]}(\mathbf{Y})) \otimes \nabla_X (\mathbf{v}^{[0]}(\mathbf{X}) + \varepsilon \mathbf{v}^{[1]}(\mathbf{Y}))] \, dV \\ &= \int_{\partial V} (\delta \mathbf{u}^{[0]}(\mathbf{X}) + \varepsilon \delta \mathbf{u}^{[1]}(\mathbf{Y})) \cdot \dot{\mathbf{t}}_0 \, dA + \int_V (\delta \mathbf{u}^{[0]}(\mathbf{X}) + \varepsilon \delta \mathbf{u}^{[1]}(\mathbf{Y})) \cdot \dot{\mathbf{f}}_0 \, dV, \quad \forall \delta \mathbf{u}^{[0]}, \delta \mathbf{u}^{[1]}. \end{aligned} \quad (20)$$

Note that by use of the chain rule and Eq. (14),

$$\begin{aligned} \nabla_X \phi(\mathbf{X}, \mathbf{Y}) &= \nabla_X \phi + \frac{\partial \mathbf{Y}}{\partial \mathbf{X}} \nabla_Y \phi \\ &= \nabla_X \phi + \frac{1}{\varepsilon} \nabla_Y \phi. \end{aligned} \quad (21)$$

Therefore,

$$\nabla_X (\mathbf{u}^{[0]}(\mathbf{X}) + \varepsilon \mathbf{u}^{[1]}(\mathbf{Y})) = \nabla_X \mathbf{u}^{[0]}(\mathbf{X}) + \nabla_Y \mathbf{u}^{[1]}(\mathbf{Y}). \quad (22)$$

Using Eq. (22) in (20) and taking the average over Y gives

$$\begin{aligned} \int_V \frac{1}{|Y|} \int_Y \mathcal{C} :: & [(\nabla_X \delta \mathbf{u}^{[0]}(\mathbf{X}) + \nabla_Y \delta \mathbf{u}^{[1]}(\mathbf{Y})) \otimes (\nabla_X \mathbf{v}^{[0]}(\mathbf{X}) + \nabla_Y \mathbf{v}^{[1]}(\mathbf{Y}))] \, dY \, dV \\ &= \int_{\partial V} (\delta \mathbf{u}^{[0]}(\mathbf{X}) + \varepsilon \delta \mathbf{u}^{[1]}(\mathbf{Y})) \cdot \dot{\mathbf{t}}_0 \, dA + \int_V (\delta \mathbf{u}^{[0]}(\mathbf{X}) + \varepsilon \delta \mathbf{u}^{[1]}(\mathbf{Y})) \cdot \dot{\mathbf{f}}_0 \, dV, \quad \forall \delta \mathbf{u}^{[0]}, \delta \mathbf{u}^{[1]}. \end{aligned} \quad (23)$$

Then, in the limit as $\varepsilon \rightarrow 0$, Eq. (23) is satisfied only if the following two equations are satisfied,

$$\begin{aligned} \frac{1}{|Y|} \int_V \int_Y \mathcal{C} &:: [\nabla_X \delta \mathbf{u}^{[0]}(\mathbf{X}) \otimes (\nabla_X \mathbf{v}^{[0]}(\mathbf{X}) + \nabla_Y \mathbf{v}^{[1]}(\mathbf{Y}))] dY dV \\ &= \int_{\partial V} \delta \mathbf{u}^{[0]}(\mathbf{X}) \cdot \dot{\mathbf{t}}_0 dA + \int_V \delta \mathbf{u}^{[0]}(\mathbf{X}) \cdot \dot{\mathbf{f}}_0 dV, \quad \forall \delta \mathbf{u}^{[0]} \end{aligned} \quad (24)$$

$$\frac{1}{|Y|} \int_V \int_Y \mathcal{C} :: [\nabla_Y \delta \mathbf{u}^{[1]}(\mathbf{Y}) \otimes (\nabla_X \mathbf{v}^{[0]}(\mathbf{X}) + \nabla_Y \mathbf{v}^{[1]}(\mathbf{Y}))] dY dV = 0, \quad \forall \delta \mathbf{u}^{[1]}. \quad (25)$$

By recourse to the finite element method, the solution of Eq. (24) is straightforward, assuming \mathcal{C} and $\mathbf{v}^{[1]}$ are known. It is then evident that due to the dependence of Eq. (25) on $\mathbf{v}^{[0]}$, Eqs. (24) and (25) are coupled and must be solved concurrently. For general problems, an iterative numerical solution scheme can be employed to handle the nonlinear system of equations together with a linearly ramped load to ensure solution convergence.

In the next section, a method is shown for solving Eq. (25) for $\mathbf{v}^{[1]}$. Then in the following section, the formulation that enables the atomistic information to be fed into Eq. (24) is derived. These two sections constitute the iteration steps that must be performed for a general application.

4. Atomistic equation

Distinct and distinguishable atoms are assumed to reside in the local level cell. By the Cauchy–Born rule (Erickson, 1984), at a point \mathbf{X} , $\mathbf{F}(\mathbf{u}^{[0]})$ is assumed to give the energy minimizing configuration of the atoms. For simplicity, we assume that the atoms are arranged in a lattice.¹ Then, the positions of the atoms \mathbf{Y} are given from the lattice coordinates \mathbf{m} by

$$\mathbf{Y}_{(\mathbf{m})} = \mathbf{m} \mathbf{e}_i : \mathbf{m} \in \mathcal{L}, \quad \mathcal{L} = \mathbb{Z}^3, \quad \mathbb{Z} \leq \mathbb{N}, \quad (26)$$

where \mathbf{e}_i are the primitive translation vectors and \mathbb{N} is the integer multiple of atoms contained in the unit cell. To avoid confusion in notation, atom labels are noted in parentheses henceforth and are not subject to the conventional summation rules associated with indicial notation. The displacement of the atoms are

$$\mathbf{q}_{(\mathbf{m})} : \mathbf{m} \in \mathcal{L}. \quad (27)$$

Upon deformation, the new positions of the atoms are given by

$$\mathbf{y}_{(\mathbf{m})} = \mathbf{Y}_{(\mathbf{m})} + \mathbf{q}_{(\mathbf{m})}. \quad (28)$$

The deformation gradient is defined by

$$\mathbf{F} = \frac{\partial \mathbf{y}}{\partial \mathbf{Y}}. \quad (29)$$

The vector separating two atoms i and j in the reference configuration is given by

$$\mathbf{R}_{(ij)} = \mathbf{Y}_{(j)} - \mathbf{Y}_{(i)}, \quad (30)$$

where $\mathbf{Y}_{(j)}$ denotes the position of atom j and $\mathbf{Y}_{(i)}$ the position of atom i . The vector separating two atoms in the deformed configuration is given by

$$\mathbf{r}_{(ij)} = \mathbf{y}_{(j)} - \mathbf{y}_{(i)}. \quad (31)$$

¹ Note that there is no restriction to perfect lattices. In fact, by using computers, general amorphous structures may also be considered as long as the assumption of the Cauchy–Born rule still applies.

Then the Cauchy–Born rule can be stated in a more precise manner by

$$\begin{aligned}\mathbf{r}_{(ij)} &= \mathbf{FY}_{(j)} - \mathbf{FY}_{(i)} \\ &= \mathbf{FR}_{(ij)}.\end{aligned}\quad (32)$$

In defect regions and through the homogenization theory via Eq. (17), the rule becomes

$$\mathbf{r}_{(ij)} = \mathbf{FR}_{(ij)} + \bar{\mathbf{r}}_{(ij)}, \quad (33)$$

where $\bar{\mathbf{r}}_{(ij)} = \mathbf{u}_{(j)}^{[1]} - \mathbf{u}_{(i)}^{[1]}$ is the additional term to account for high energy regions.

For the energy associated with the deformation of the atoms, we use a modified form of the so-called Potential II parameterization of the Tersoff–Brenner potential (Tersoff, 1988; Brenner, 1990). It takes the form

$$\mathcal{W} = \frac{1}{N} [E_b(\mathbf{Y} + \mathbf{q}) - E_b(\mathbf{Y})], \quad (34)$$

where \mathcal{W} is the energy density of the frozen system, N is the number of atoms in the cell, and E_b is the binding energy given for a pure carbon system by

$$E_b(\mathbf{r}) = \sum_i \sum_{j(>i)} [V_R(r_{(ij)}) - \bar{B}V_A(r_{(ij)})], \quad (35)$$

$$\bar{B} = \frac{1}{2}(B_{(ij)} + B_{(ji)}), \quad (36)$$

$$V_R(r) = \frac{f_{(ij)}(r)D^{(e)}}{(S-1)} e^{-\sqrt{2S}\beta(r-R^{(e)})}, \quad (37)$$

$$V_A(r) = \frac{f_{(ij)}(r)D^{(e)}S}{(S-1)} e^{-\sqrt{\frac{2}{3}}\beta(r-R^{(e)})}, \quad (38)$$

$$f_{(ij)}(r) = \begin{cases} 1, & r < R^{(1)}, \\ \frac{1}{2} \left\{ 1 + \cos \left[\frac{\pi(r - R^{(1)})}{(r - R^{(2)})} \right] \right\}, & R^{(1)} < r < R^{(2)}, \\ 0, & r > R^{(2)}, \end{cases} \quad (39)$$

$$B_{(ij)} = \left[1 + \sum_{k \neq i, j} G(\theta_{(ijk)}) f_{(ik)}(r_{(ik)}) \right]^{-\delta}, \quad (40)$$

$$G(\theta) = a_0 \left\{ 1 + \frac{c_0^2}{d_0^2} - \frac{c_0^2}{d_0^2 + (1 + \cos \theta)^2} \right\}, \quad (41)$$

with the constants given in Table 1. The modification in this work comes by way of omitting the extra bond-order term in (Brenner, 1990), which is primarily used for problems involving changes in coordination numbers. We therefore presently restrict our consideration to classes of deformation involving no change in coordination.

Given that the energy can be written as a function of the atom displacements, Eq. (25) can be expressed in a form conducive to atom representations. We equate $\mathbf{v}^{[1]}$ to the rate of atom displacement and attempt to solve the equivalent form

Table 1

Parameters for Tersoff–Brenner potential

$R^{(e)}$	1.39 Å
$D^{(e)}$	6.0 eV
S	1.22
β	2.1 Å
δ	0.5
$R^{(1)}$	1.7 Å
$R^{(2)}$	2.0 Å
a_0	0.00020813
c_0^2	330 ²
d_0^2	3.5 ²

$$\frac{\partial}{\partial Y_j} \mathcal{C}_{ijkl} \frac{\partial v_k^{[1]}}{\partial Y_l} = - \frac{\partial \mathcal{C}_{ijkl}}{\partial Y_j} \frac{\partial v_k^{[0]}}{\partial X_l} \quad (42)$$

under periodic boundary conditions. The solution to Eq. (42) is found as the zero of $\partial \mathcal{R}$ in the equation

$$\partial \mathcal{R} = \mathcal{K} \mathbf{v}^{[1]} - \mathcal{D} \cdot \nabla_0 \mathbf{v}^{[0]}(\mathbf{x}), \quad (43)$$

where \mathcal{K} is the $N \times N$ Hessian and is given by

$$\mathcal{K} = \frac{\partial^2 \mathcal{W}}{\partial \mathbf{q} \partial \mathbf{q}}, \quad (44)$$

where \mathbf{q} is the vector of atom displacements of size $3N$ (in three dimensions) and \mathcal{D} is a third order unsymmetric tensor that is obtained from the first derivative of the Euler–Lagrange equation with respect to the local deformation gradient given by

$$\mathcal{D} = - \frac{\partial^2 \mathcal{W}}{\partial \mathbf{q} \partial \mathbf{F}}. \quad (45)$$

The size of \mathcal{D} depends on the dimensionality of the problem. In three dimensions, it can be expressed as an $N \times 9$ matrix, where 9 corresponds to the number of independent components of \mathbf{F} .

5. Multiscale equation

Once Eq. (43) has been solved for $\mathbf{v}^{[1]}$, the remaining task is to formulate a tractable global scale boundary value problem. The key distinction between this investigation and conventional continuum formulations, such as hyperelasticity, is the conspicuous incorporation of $\mathbf{v}^{[1]}$, a fine-scale/atomistic quantity, in the global scale equations, and the definition of the material property tensor completely in terms of atomistic variables.

We return to Eq. (24), recognizing that $\mathbf{v}^{[1]}$ is now known. Incorporating the definition for the first Lagrangian elasticity tensor from Eq. (9) yields

$$\begin{aligned} \frac{1}{|Y|} \int_V \int_Y \frac{\partial^2 \mathcal{W}}{\partial \mathbf{F} \partial \mathbf{F}} &:: [\nabla_X \boldsymbol{\delta} \mathbf{u}^{[0]}(\mathbf{X}) \otimes (\nabla_X \mathbf{v}^{[0]}(\mathbf{X}) + \nabla_Y \mathbf{v}^{[1]}(\mathbf{Y}))] dY dV \\ &= \int_{\partial V} \boldsymbol{\delta} \mathbf{u}^{[0]}(\mathbf{X}) \cdot \dot{\mathbf{t}}_0 dA + \int_V \boldsymbol{\delta} \mathbf{u}^{[0]}(\mathbf{X}) \cdot \dot{\mathbf{f}}_0 dV, \quad \forall \boldsymbol{\delta} \mathbf{u}^{[0]}. \end{aligned} \quad (46)$$

Then, using the definition of \mathbf{F} in Eq. (1) and assuming a first-order Taylor series representation for the time derivative gives,

$$\begin{aligned}
& \frac{1}{|Y|} \int_V \int_Y \frac{\partial^2 \mathcal{W}}{\partial \mathbf{F} \partial \mathbf{F}} : (\nabla_X \boldsymbol{\delta} \mathbf{u}^{[0]}(\mathbf{X}) \otimes \nabla_X \mathbf{v}^{[0]}(\mathbf{X})) dY dV \\
&= \int_{\partial V} \boldsymbol{\delta} \mathbf{u}^{[0]}(\mathbf{X}) \cdot \mathbf{t}_0 dA + \int_V \boldsymbol{\delta} \mathbf{u}^{[0]}(\mathbf{X}) \cdot \mathbf{f}_0 dV \\
&\quad - \frac{1}{|Y|} \int_V \int_Y \frac{\partial^2 \mathcal{W}}{\partial \mathbf{F} \partial \mathbf{q}} : (\nabla_X \boldsymbol{\delta} \mathbf{u}^{[0]}(\mathbf{X}) \otimes \mathbf{v}^{[1]}(\mathbf{Y})) dY dV, \quad \forall \boldsymbol{\delta} \mathbf{u}^{[0]},
\end{aligned} \tag{47}$$

where there is now a double contraction on $\nabla_X \boldsymbol{\delta} \mathbf{u}^{[0]}$ and a single contraction on $\mathbf{v}^{[1]}$ in the last expression of Eq. (47). The solution to Eq. (47) yields $\mathbf{v}^{[0]}$. It is noteworthy that the last term is zero when the energy distribution over Y is constant, i.e., when the atom arrangement forms a perfect lattice. This reduces the problem to a classical harmonic approximation where the first Lagrangian elasticity tensor is assumed to model the material behavior. In Eq. (47), the last term serves as a corrective force in regions of highly energetic atoms, i.e., nonlocal regions, to account for defects and lattice inhomogeneities.

6. The Euler–Lagrange equations and the Hessian

In this section, the analytic forms of the Euler–Lagrange equations and Hessian are derived for a general potential. The lengthy algebra typically needed to obtain Eqs. (44) and (45) for the specific case of the Tersoff–Brenner potential are shown in greater detail in Appendix A, and only general forms are derived here. The Euler–Lagrange equation is the first derivative of the Lagrangian with respect to the degrees of freedom. In this problem, the Lagrangian is the negative of the atomistic energy density, which we presently assume is equivalent to the free energy at zero temperature. The Euler–Lagrange equation is therefore given by

$$\begin{aligned}
\mathcal{E} &= \frac{\partial \mathcal{W}}{\partial \mathbf{q}_{(m)}} \\
&= \frac{1}{N} \frac{\partial E_b}{\partial \mathbf{q}_{(m)}},
\end{aligned} \tag{48}$$

and using the chain rule for derivatives, it is

$$\begin{aligned}
\mathcal{E} &= \frac{1}{N} \frac{\partial E_b}{\partial \mathbf{q}_{(m)}} \\
&= \frac{1}{N} \left(\frac{\partial E_b}{\partial \mathbf{r}_{(ij)}} \cdot \frac{\partial \mathbf{r}_{(ij)}}{\partial \mathbf{q}_{(m)}} + \frac{\partial E_b}{\partial \mathbf{r}_{(ik)}} \cdot \frac{\partial \mathbf{r}_{(ik)}}{\partial \mathbf{q}_{(m)}} + \frac{\partial E_b}{\partial \mathbf{r}_{(jk)}} \cdot \frac{\partial \mathbf{r}_{(jk)}}{\partial \mathbf{q}_{(m)}} \right).
\end{aligned} \tag{49}$$

Here, we have implicitly assumed that there are three independent atomic position vectors. One can show quite easily that there are in fact only two by using the relationship $\mathbf{r}_{(jk)} = \mathbf{r}_{(ik)} - \mathbf{r}_{(ij)}$.

The Hessian is obtained by taking an additional derivative of the Euler–Lagrange equations. Specifically, we again make use of the chain rule to obtain

$$\begin{aligned}
\mathcal{K} &= \frac{\partial^2 \mathcal{W}}{\partial \mathbf{q}_{(n)} \partial \mathbf{q}_{(m)}} = \frac{1}{N} \frac{\partial^2 E_b}{\partial \mathbf{q}_{(n)} \partial \mathbf{q}_{(m)}} \\
&= \frac{1}{N} \left[\frac{\partial^2 E_b}{\partial \mathbf{r}_{(ij)} \partial \mathbf{r}_{(ij)}} : \left(\frac{\partial \mathbf{r}_{(ij)}}{\partial \mathbf{q}_{(n)}} \otimes \frac{\partial \mathbf{r}_{(ij)}}{\partial \mathbf{q}_{(m)}} \right) + \frac{\partial^2 E_b}{\partial \mathbf{r}_{(ij)} \partial \mathbf{r}_{(ik)}} : \left(\frac{\partial \mathbf{r}_{(ij)}}{\partial \mathbf{q}_{(n)}} \otimes \frac{\partial \mathbf{r}_{(ik)}}{\partial \mathbf{q}_{(m)}} \right) + \frac{\partial^2 E_b}{\partial \mathbf{r}_{(ik)} \partial \mathbf{r}_{(ij)}} : \left(\frac{\partial \mathbf{r}_{(ik)}}{\partial \mathbf{q}_{(n)}} \otimes \frac{\partial \mathbf{r}_{(ij)}}{\partial \mathbf{q}_{(m)}} \right) \right. \\
&\quad + \frac{\partial^2 E_b}{\partial \mathbf{r}_{(ik)} \partial \mathbf{r}_{(ik)}} : \left(\frac{\partial \mathbf{r}_{(ik)}}{\partial \mathbf{q}_{(n)}} \otimes \frac{\partial \mathbf{r}_{(ik)}}{\partial \mathbf{q}_{(m)}} \right) + \frac{\partial^2 E_b}{\partial \mathbf{r}_{(jk)} \partial \mathbf{r}_{(jk)}} : \left(\frac{\partial \mathbf{r}_{(jk)}}{\partial \mathbf{q}_{(n)}} \otimes \frac{\partial \mathbf{r}_{(jk)}}{\partial \mathbf{q}_{(m)}} \right) + \frac{\partial^2 E_b}{\partial \mathbf{r}_{(ij)} \partial \mathbf{r}_{(jk)}} : \left(\frac{\partial \mathbf{r}_{(ij)}}{\partial \mathbf{q}_{(n)}} \otimes \frac{\partial \mathbf{r}_{(jk)}}{\partial \mathbf{q}_{(m)}} \right) \\
&\quad + \frac{\partial^2 E_b}{\partial \mathbf{r}_{(jk)} \partial \mathbf{r}_{(ij)}} : \left(\frac{\partial \mathbf{r}_{(jk)}}{\partial \mathbf{q}_{(n)}} \otimes \frac{\partial \mathbf{r}_{(ij)}}{\partial \mathbf{q}_{(m)}} \right) + \frac{\partial^2 E_b}{\partial \mathbf{r}_{(ik)} \partial \mathbf{r}_{(jk)}} : \left(\frac{\partial \mathbf{r}_{(ik)}}{\partial \mathbf{q}_{(n)}} \otimes \frac{\partial \mathbf{r}_{(jk)}}{\partial \mathbf{q}_{(m)}} \right) \\
&\quad \left. + \frac{\partial^2 E_b}{\partial \mathbf{r}_{(jk)} \partial \mathbf{r}_{(ik)}} : \left(\frac{\partial \mathbf{r}_{(jk)}}{\partial \mathbf{q}_{(n)}} \otimes \frac{\partial \mathbf{r}_{(ik)}}{\partial \mathbf{q}_{(m)}} \right) \right]. \tag{50}
\end{aligned}$$

Second derivatives of the interatom vectors are zero, i.e.,

$$\frac{\partial^2 \mathbf{r}_{(ij)}}{\partial \mathbf{q}_{(m)} \partial \mathbf{q}_{(n)}} = \frac{\partial^2}{\partial \mathbf{q}_{(m)} \partial \mathbf{q}_{(n)}} (\mathbf{Y}_{(j)} + \mathbf{q}_{(j)} - \mathbf{Y}_{(i)} - \mathbf{q}_{(i)}) \tag{51}$$

$$= \mathbf{0} \quad \forall (m, n). \tag{52}$$

Next, the appropriate right-hand side expressions are derived for Eqs. (43) and (45). This involves the use of the chain rule again to obtain

$$\begin{aligned}
\frac{\partial^2 \mathcal{W}}{\partial \mathbf{q}_{(m)} \partial \mathbf{F}} &= \frac{1}{N} \left[\frac{\partial^2 E_b}{\partial \mathbf{r}_{(ij)} \partial \mathbf{r}_{(ij)}} : \left(\frac{\partial \mathbf{r}_{(ij)}}{\partial \mathbf{F}} \otimes \frac{\partial \mathbf{r}_{(ij)}}{\partial \mathbf{q}_{(m)}} \right) + \frac{\partial^2 E_b}{\partial \mathbf{r}_{(ij)} \partial \mathbf{r}_{(ik)}} : \left(\frac{\partial \mathbf{r}_{(ik)}}{\partial \mathbf{F}} \otimes \frac{\partial \mathbf{r}_{(ij)}}{\partial \mathbf{q}_{(m)}} \right) + \frac{\partial^2 E_b}{\partial \mathbf{r}_{(ik)} \partial \mathbf{r}_{(ij)}} : \left(\frac{\partial \mathbf{r}_{(ij)}}{\partial \mathbf{F}} \otimes \frac{\partial \mathbf{r}_{(ik)}}{\partial \mathbf{q}_{(m)}} \right) \right. \\
&\quad + \frac{\partial^2 E_b}{\partial \mathbf{r}_{(ik)} \partial \mathbf{r}_{(ik)}} : \left(\frac{\partial \mathbf{r}_{(ik)}}{\partial \mathbf{F}} \otimes \frac{\partial \mathbf{r}_{(ik)}}{\partial \mathbf{q}_{(m)}} \right) + \frac{\partial^2 E_b}{\partial \mathbf{r}_{(ij)} \partial \mathbf{r}_{(jk)}} : \left(\frac{\partial \mathbf{r}_{(jk)}}{\partial \mathbf{F}} \otimes \frac{\partial \mathbf{r}_{(ij)}}{\partial \mathbf{q}_{(m)}} \right) + \frac{\partial^2 E_b}{\partial \mathbf{r}_{(jk)} \partial \mathbf{r}_{(ij)}} : \left(\frac{\partial \mathbf{r}_{(ij)}}{\partial \mathbf{F}} \otimes \frac{\partial \mathbf{r}_{(jk)}}{\partial \mathbf{q}_{(m)}} \right) \\
&\quad \left. + \frac{\partial^2 E_b}{\partial \mathbf{r}_{(ik)} \partial \mathbf{r}_{(jk)}} : \left(\frac{\partial \mathbf{r}_{(jk)}}{\partial \mathbf{F}} \otimes \frac{\partial \mathbf{r}_{(ik)}}{\partial \mathbf{q}_{(m)}} \right) + \frac{\partial^2 E_b}{\partial \mathbf{r}_{(jk)} \partial \mathbf{r}_{(ik)}} : \left(\frac{\partial \mathbf{r}_{(ik)}}{\partial \mathbf{F}} \otimes \frac{\partial \mathbf{r}_{(jk)}}{\partial \mathbf{q}_{(m)}} \right) + \frac{\partial^2 E_b}{\partial \mathbf{r}_{(jk)} \partial \mathbf{r}_{(jk)}} : \left(\frac{\partial \mathbf{r}_{(jk)}}{\partial \mathbf{F}} \otimes \frac{\partial \mathbf{r}_{(jk)}}{\partial \mathbf{q}_{(m)}} \right) \right], \tag{53}
\end{aligned}$$

and by definition,

$$\frac{\partial \mathbf{r}_{(ij)}}{\partial \mathbf{F}} = \mathbf{R}_{(ij)} \quad \text{and} \quad \frac{\partial \mathbf{r}_{(ik)}}{\partial \mathbf{F}} = \mathbf{R}_{(ik)}. \tag{54}$$

Finally, we use a similar approach to define the first Lagrangian elasticity tensor. This is the traditional way of estimating the elastic properties of a solid. Using the chain rule once again gives,

$$\begin{aligned}
\frac{\partial^2 \mathcal{W}}{\partial \mathbf{F} \partial \mathbf{F}} &= \frac{1}{N} \left[\frac{\partial^2 E_b}{\partial \mathbf{r}_{(ij)} \partial \mathbf{r}_{(ij)}} : \left(\frac{\partial \mathbf{r}_{(ij)}}{\partial \mathbf{F}} \otimes \frac{\partial \mathbf{r}_{(ij)}}{\partial \mathbf{F}} \right) + \frac{\partial^2 E_b}{\partial \mathbf{r}_{(ij)} \partial \mathbf{r}_{(ik)}} : \left(\frac{\partial \mathbf{r}_{(ik)}}{\partial \mathbf{F}} \otimes \frac{\partial \mathbf{r}_{(ij)}}{\partial \mathbf{F}} \right) + \frac{\partial^2 E_b}{\partial \mathbf{r}_{(ik)} \partial \mathbf{r}_{(ij)}} : \left(\frac{\partial \mathbf{r}_{(ij)}}{\partial \mathbf{F}} \otimes \frac{\partial \mathbf{r}_{(ik)}}{\partial \mathbf{F}} \right) \right. \\
&\quad + \frac{\partial^2 E_b}{\partial \mathbf{r}_{(ik)} \partial \mathbf{r}_{(ik)}} : \left(\frac{\partial \mathbf{r}_{(ik)}}{\partial \mathbf{F}} \otimes \frac{\partial \mathbf{r}_{(ik)}}{\partial \mathbf{F}} \right) + \frac{\partial^2 E_b}{\partial \mathbf{r}_{(ij)} \partial \mathbf{r}_{(jk)}} : \left(\frac{\partial \mathbf{r}_{(jk)}}{\partial \mathbf{F}} \otimes \frac{\partial \mathbf{r}_{(ij)}}{\partial \mathbf{F}} \right) + \frac{\partial^2 E_b}{\partial \mathbf{r}_{(jk)} \partial \mathbf{r}_{(ij)}} : \left(\frac{\partial \mathbf{r}_{(ij)}}{\partial \mathbf{F}} \otimes \frac{\partial \mathbf{r}_{(jk)}}{\partial \mathbf{F}} \right) \\
&\quad \left. + \frac{\partial^2 E_b}{\partial \mathbf{r}_{(ik)} \partial \mathbf{r}_{(jk)}} : \left(\frac{\partial \mathbf{r}_{(jk)}}{\partial \mathbf{F}} \otimes \frac{\partial \mathbf{r}_{(ik)}}{\partial \mathbf{F}} \right) + \frac{\partial^2 E_b}{\partial \mathbf{r}_{(jk)} \partial \mathbf{r}_{(ik)}} : \left(\frac{\partial \mathbf{r}_{(ik)}}{\partial \mathbf{F}} \otimes \frac{\partial \mathbf{r}_{(jk)}}{\partial \mathbf{F}} \right) + \frac{\partial^2 E_b}{\partial \mathbf{r}_{(jk)} \partial \mathbf{r}_{(jk)}} : \left(\frac{\partial \mathbf{r}_{(jk)}}{\partial \mathbf{F}} \otimes \frac{\partial \mathbf{r}_{(jk)}}{\partial \mathbf{F}} \right) \right]. \tag{55}
\end{aligned}$$

The first Lagrangian elasticity tensor is used in Eq. (47), whose solution gives $\mathbf{v}^{[0]}$. In a perfect lattice, Eq. (55) provides the only atomistic material information needed to solve the macroscopic continuum problem. The next section illustrates this by showing that the perturbation is zero for a uniform crystal.

7. Example problems

7.1. Example I: perfect 1-D atomic lattice

To illustrate the calculation, a 1-D analytical example is presented. The Tersoff–Brenner potential is used to represent the energetics of a 1-D single-species chain of carbon atoms. The objective here is to solve Eqs. (42) and (43) for $\mathbf{v}^{[1]}$ and demonstrate a simple case of a perfect lattice using this method.

One atom comprises the periodic unit cell, but to account for the effects of triples, two “fictitious” atoms are assumed to extend beyond the boundaries of the cell on each side as illustrated in Fig. 1. Periodic conditions apply at the cell boundaries. The equilibrium lattice constant for the chain is $r_0 = 1.86868 \text{ \AA}$.

The following two conditions stem from the 1-D assumption,

$$\begin{aligned} \theta &= \pi, \\ R^{(1)} &< r < R^{(2)}. \end{aligned} \quad (56)$$

This simplifies the expressions in Appendix A. The resulting Hessian for three arbitrary colinear atoms (i, j, k) is obtained as

$$[\mathcal{K}^{(ijk)}] = \begin{bmatrix} \mathcal{K}_{11}^{(ijk)} & \mathcal{K}_{12}^{(ijk)} & \mathcal{K}_{13}^{(ijk)} \\ \mathcal{K}_{21}^{(ijk)} & \mathcal{K}_{22}^{(ijk)} & \mathcal{K}_{23}^{(ijk)} \\ \mathcal{K}_{31}^{(ijk)} & \mathcal{K}_{32}^{(ijk)} & \mathcal{K}_{33}^{(ijk)} \end{bmatrix}, \quad (57)$$

where $\mathcal{K}_{mn}^{(ijk)} = \mathcal{K}_{nm}^{(ijk)}$ and the terms are defined by

$$\mathcal{K}_{11}^{(ijk)} = V_R'' - \bar{B}V_A'' + a_0\delta V_A' B_{(ij)}^{1+\frac{1}{\delta}} f'_{(ik)} + \frac{\delta}{2}(\delta+1)V_A B_{(ij)}^{1+\frac{2}{\delta}} (a_0 f'_{(ik)})^2 + \frac{a_0\delta}{2}V_A B_{(ij)}^{1+\frac{1}{\delta}} f''_{(ik)}, \quad (58)$$

$$\mathcal{K}_{12}^{(ijk)} = -V_R'' + \bar{B}V_A'' - \frac{a_0\delta}{2}V_A' B_{(ij)}^{1+\frac{1}{\delta}} f'_{(ik)}, \quad (59)$$

$$\mathcal{K}_{13}^{(ijk)} = -\frac{a_0\delta}{2}V_A' B_{(ij)}^{1+\frac{1}{\delta}} f'_{(ik)} - \frac{\delta}{2}(\delta+1)V_A B_{(ij)}^{1+\frac{2}{\delta}} (a_0 f'_{(ik)})^2 - \frac{a_0\delta}{2}V_A B_{(ij)}^{1+\frac{1}{\delta}} f''_{(ik)}, \quad (60)$$

$$\mathcal{K}_{22}^{(ijk)} = V_R'' - \bar{B}V_A'', \quad (61)$$

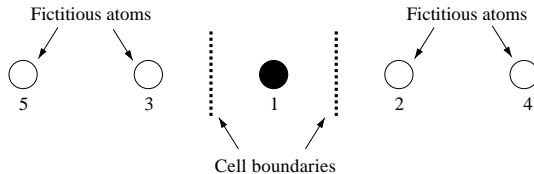


Fig. 1. Unit cell of the 1-D carbon chain. The atoms are labeled by identifying numbers.

$$\mathcal{K}_{23}^{(ijk)} = \frac{a_0 \delta}{2} V_A' B_{(ij)}^{1+\frac{1}{\delta}} f'_{(ik)}, \quad (62)$$

$$\mathcal{K}_{33}^{(ijk)} = \frac{\delta}{2} (\delta + 1) V_A B_{(ij)}^{1+\frac{2}{\delta}} (a_0 f'_{(ik)})^2 + \frac{a_0 \delta}{2} V_A B_{(ij)}^{1+\frac{1}{\delta}} f''_{(ik)}. \quad (63)$$

Upon assembly of the two unique pairs (31,12) and their associated triples (123,132) in Fig. 1, the final assembled Hessian of the global system is given by the matrix,

$$[\mathcal{K}] = \begin{bmatrix} \mathcal{K}_{11} & \mathcal{K}_{12} & \mathcal{K}_{13} \\ \mathcal{K}_{21} & \mathcal{K}_{22} & \mathcal{K}_{23} \\ \mathcal{K}_{31} & \mathcal{K}_{32} & \mathcal{K}_{33} \end{bmatrix}, \quad (64)$$

which is assembled through the operation,

$$[\mathcal{K}] = \bigsqcup_{(m)} \bigsqcup_{(n)}^{(i,j,k)} [\mathcal{K}^{(ijk)}] = \mathcal{K}_{mn}, \quad (65)$$

where \bigsqcup is the addition operator over all unique pair and triple combinations of (i, j, k) and (m) and (n) are displacement degrees of freedom for each atom. In Eq. (65), $[\mathcal{K}]$ is symmetric once again, and its components are obtained in detail for the problem shown in Fig. 1 as follows:

$$\mathcal{K}_{11} = \mathcal{K}_{11}^{(123)} + \mathcal{K}_{22}^{(315)} + \mathcal{K}_{33}^{(241)}, \quad (66)$$

$$\mathcal{K}_{12} = \mathcal{K}_{12}^{(123)} + \mathcal{K}_{13}^{(241)}, \quad (67)$$

$$\mathcal{K}_{13} = \mathcal{K}_{13}^{(123)} + \mathcal{K}_{12}^{(315)}, \quad (68)$$

$$\mathcal{K}_{22} = \mathcal{K}_{22}^{(123)} + \mathcal{K}_{11}^{(241)}, \quad (69)$$

$$\mathcal{K}_{23} = \mathcal{K}_{23}^{(123)}, \quad (70)$$

$$\mathcal{K}_{33} = \mathcal{K}_{33}^{(123)} + \mathcal{K}_{11}^{(315)}. \quad (71)$$

This constitutes the stiffness matrix \mathcal{K} in Eq. (43).

The next step is to calculate the right-hand side of Eq. (42), which is equivalent to calculating \mathcal{D} and multiplying by the global rate of the deformation gradient. Using Eqs. (45) and (53), the right-hand side for three colinear atoms (i, j, k) is obtained as

$$\{\mathcal{D}^{(ijk)}\} = \left\{ \begin{array}{c} \mathcal{D}_1^{(ijk)} \\ \mathcal{D}_2^{(ijk)} \\ \mathcal{D}_3^{(ijk)} \end{array} \right\}, \quad (72)$$

where the components are defined by

$$\begin{aligned}\mathcal{D}_1^{(ijk)} &= R_{(ij)}(V_R'' - \bar{B}V_A'') + (R_{(ik)} - R_{(ij)})\left(\frac{a_0\delta}{2}V_A'B_{(ij)}^{1+\frac{1}{\delta}}f'_{(ik)}\right) \\ &+ R_{(ik)}\left(\frac{\delta}{2}(\delta+1)V_A'B_{(ij)}^{1+\frac{2}{\delta}}\left(a_0f'_{(ik)}\right)^2 + \frac{a_0\delta}{2}V_A'B_{(ij)}^{1+\frac{1}{\delta}}f''_{(ik)}\right),\end{aligned}\quad (73)$$

$$\mathcal{D}_2^{(ijk)} = -R_{(ij)}(V_R'' - \bar{B}V_A'') - R_{(ik)}\left(\frac{a_0\delta}{2}V_A'B_{(ij)}^{1+\frac{1}{\delta}}f'_{(ik)}\right), \quad (74)$$

$$\mathcal{D}_3^{(ijk)} = -R_{(ij)}\left(\frac{a_0\delta}{2}V_A'B_{(ij)}^{1+\frac{1}{\delta}}f'_{(ik)}\right) - R_{(ik)}\left(\frac{\delta}{2}(\delta+1)V_A'B_{(ij)}^{1+\frac{2}{\delta}}\left(a_0f'_{(ik)}\right)^2 + \frac{a_0\delta}{2}V_A'B_{(ij)}^{1+\frac{1}{\delta}}f''_{(ik)}\right). \quad (75)$$

As earlier, the assembly operation

$$\{\mathcal{D}\} = \bigsqcup_{(m)}^{(i,j,k)} \{\mathcal{D}^{(ijk)}\} = \mathcal{D}_m, \quad (76)$$

yields the right-hand side of the global system given by,

$$\{\mathcal{D}\} = \begin{Bmatrix} \mathcal{D}_1 \\ \mathcal{D}_2 \\ \mathcal{D}_3 \end{Bmatrix}, \quad (77)$$

where the components are

$$\mathcal{D}_1 = \mathcal{D}_1^{(123)} + \mathcal{D}_2^{(315)} + \mathcal{D}_3^{(241)}, \quad (78)$$

$$\mathcal{D}_2 = \mathcal{D}_2^{(123)} + \mathcal{D}_1^{(241)}, \quad (79)$$

$$\mathcal{D}_3 = \mathcal{D}_3^{(123)} + \mathcal{D}_1^{(315)}. \quad (80)$$

Under the assumption of a 1-D perfect lattice, we have $R_{(ij)} = R_{(ik)}$ and, consequently, $\mathcal{D}_1 = 0$. Then, we can satisfy the periodicity condition and the rigid body constraint by setting $v_{(2)}^{[1]} = v_{(3)}^{[1]} = 0$. The solution is therefore

$$v_{(1)}^{[1]} = v_{(2)}^{[1]} = v_{(3)}^{[1]} = 0. \quad (81)$$

In light of Eq. (81), the last term in Eq. (47) is zero, and the material properties are obtained from the atomistic energy density solely through Eq. (55). This result shows that in a defect-free lattice, the homogenization method coincides with the conventional atomistic hyperelasticity problem. The next section shows an example in which a defect causes an inhomogeneous energy distribution, leading to a situation where homogenization is needed to average out the energy.

7.2. Example II: 1-D atomic lattice with defect

Consider the problem shown in Fig. 2, where the center atom is displaced by a distance L from its original energy minimizing configuration. This displacement of the center atom constitutes the defect.

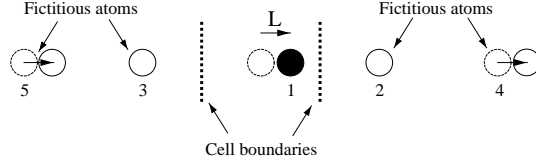


Fig. 2. Unit cell of 1-D carbon chain with periodic defect.

With this change, the key stiffness matrix term in Eq. (66) is now

$$\begin{aligned} \mathcal{K}_{11} = & V''_{R_{(12)}} - \bar{B}_{(12)} V''_{A_{(12)}} + a_0 \delta V'_{A_{(12)}} B_{(12)}^{1+\frac{1}{\delta}} f'_{(13)} + \frac{\delta}{2} (\delta + 1) V_{A_{(12)}} B_{(12)}^{1+\frac{2}{\delta}} (a_0 f'_{(13)})^2 + \frac{a_0 \delta}{2} V_{A_{(12)}} B_{(12)}^{1+\frac{1}{\delta}} f''_{(13)} \\ & + V''_{R_{(13)}} - \bar{B}_{(13)} V''_{A_{(13)}} + a_0 \delta V'_{A_{(13)}} B_{(13)}^{1+\frac{1}{\delta}} f'_{(12)} + \frac{\delta}{2} (\delta + 1) V_{A_{(13)}} B_{(13)}^{1+\frac{2}{\delta}} (a_0 f'_{(12)})^2 + \frac{a_0 \delta}{2} V_{A_{(13)}} B_{(13)}^{1+\frac{1}{\delta}} f''_{(12)}, \end{aligned} \quad (82)$$

and likewise, Eq. (78) is now

$$\begin{aligned} \mathcal{D}_1 = & R_{(12)} (V''_{R_{(12)}} - \bar{B}_{(12)} V''_{A_{(12)}}) + (R_{(13)} - R_{(12)}) \left(\frac{a_0 \delta}{2} V'_{A_{(12)}} B_{(12)}^{1+\frac{1}{\delta}} f'_{(13)} \right) + R_{(13)} \left(\frac{\delta}{2} (\delta + 1) V_{A_{(12)}} B_{(12)}^{1+\frac{2}{\delta}} (a_0 f'_{(13)})^2 \right. \\ & \left. + \frac{a_0 \delta}{2} V_{A_{(12)}} B_{(12)}^{1+\frac{1}{\delta}} f''_{(13)} \right) - R_{(13)} (V''_{R_{(13)}} - \bar{B}_{(13)} V''_{A_{(13)}}) - (R_{(12)} - R_{(13)}) \left(\frac{a_0 \delta}{2} V'_{A_{(13)}} B_{(13)}^{1+\frac{1}{\delta}} f'_{(12)} \right) \\ & - R_{(12)} \left(\frac{\delta}{2} (\delta + 1) V_{A_{(13)}} B_{(13)}^{1+\frac{2}{\delta}} (a_0 f'_{(12)})^2 + \frac{a_0 \delta}{2} V_{A_{(13)}} B_{(13)}^{1+\frac{1}{\delta}} f''_{(12)} \right), \end{aligned} \quad (83)$$

where $R_{(12)} = r_0 - L$ and $R_{(13)} = r_0 + L$. Then, solving Eq. (43) under periodic boundary conditions gives

$$v_1^{[1]} = \frac{\mathcal{D}_1}{\mathcal{K}_1} \frac{\partial v^{[0]}}{\partial x}, \quad v_2^{[1]} = v_3^{[1]} = 0. \quad (84)$$

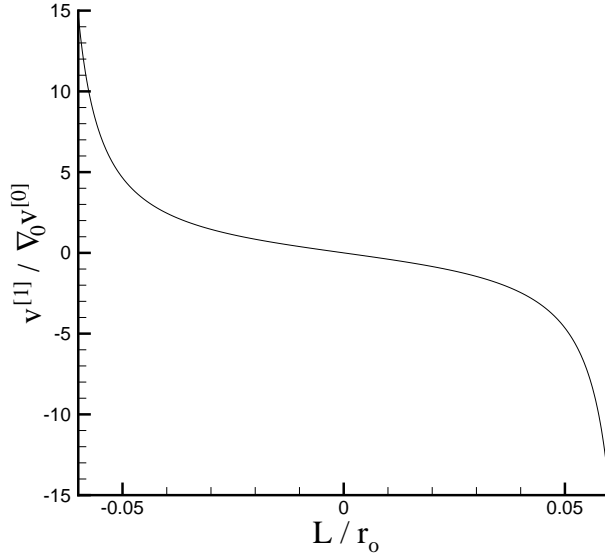


Fig. 3. Distribution of $v^{[1]} / \nabla_0 v^{[0]}$ solution as a function of the defect size L .

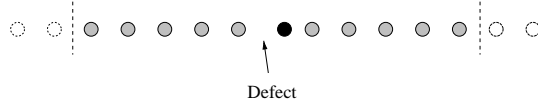


Fig. 4. Larger chain of atoms in perfect arrangement around the defect region decreases the defect density.

The $v^{[1]} / \nabla_0 v^{[0]}$ solution as a function of L/r_0 is shown in Fig. 3. As expected, the solution has symmetry about the origin and grows asymptotically larger as the size of the defect (L) grows closer to the cut-off radii. We intentionally avoid larger defects due to the nonconvex structure of the energy well associated with the Tersoff–Brenner potential. This generally leads to unphysical discontinuities in the perturbation velocity ($v^{[1]}$) due to discontinuous second derivatives of the atomistic energy with respect to the defect size. This is attributable to the construction of the empirical potential in Eqs. (35)–(41), which is suited, by design, for systems where nearest neighbor atoms, even in defect regions, are within the cut-off radius $R^{(2)}$.

It is also noteworthy that arbitrary defect densities can be treated by appropriate modification of the unit cell. In most cases, one can tailor the desired density by increasing the size of the unit cell and performing the summations and the assembly of the atomistic discrete equations over more atoms. Fig. 4 illustrates this idea for the 1-D carbon chain.

Numerical experiments show that as the size of the unit cell increases, the perturbative displacement has a sharp discontinuity at the defect. Fig. 5 shows this nonlocal behavior as the number of atoms increases. The problem is of a single defect in chains of increasing size. The defect magnitude is held fixed at $L/r_0 = 0.01$. The nonlocal discontinuity of the perturbative velocity qualitatively agrees with traditional displacement jumps that occur at dislocation cores. The discontinuity indicates that the material property at the defect ($\partial^2 W / \partial \mathbf{F} \partial \mathbf{F}$) is modified by the last term in Eq. (47), an amount proportional to $v^{[1]}$ that serves as a correcting force for the nonlocal effect.

Although the primary details of the method have been demonstrated in these two examples, the method can be extended to consider the multiscale problem shown in Eq. (47) for more general cases involving self-consistent solutions with Eq. (43) as in the next section.

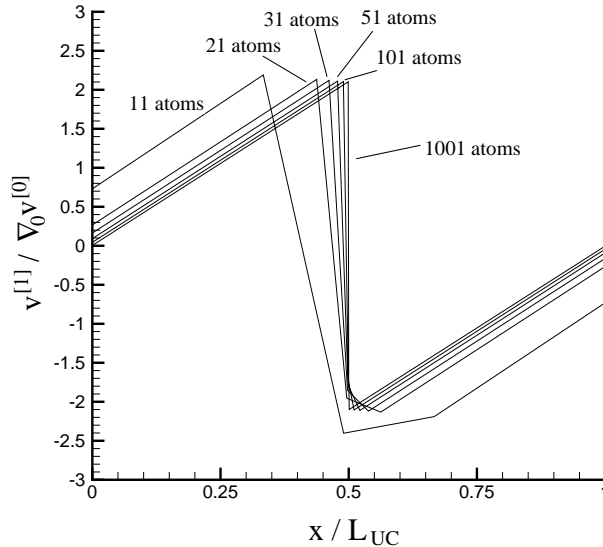


Fig. 5. Distribution of $v^{[1]} / \nabla_0 v^{[0]}$ along unit cell length for varying number of atoms ($L/r_0 = 0.01$).

7.3. Example III: 2-D graphene with defect

The method can be generalized to multiaxial problems. In this example, we consider graphene with three types of point defects: interstitial, equilibrium point vacancy and saddle point vacancy. The atom positions around the point defects were first computed using quenched molecular dynamics. These are illustrated in Fig. 6 together with the original defect-free configuration. Similar defect structures have been encountered both numerically and experimentally (Kaxiras and Pandey, 1988; Hjort and Stafström, 2000; Krasheninnikov et al., 2002).

The effective elastic constants for the defect-free case were in the form of the first Lagrangian elasticity tensor (55), which compare reasonably with experimental results. Using the second derivative of the Tersoff–Brenner potential, the bulk values (in units eV/atom) for graphene were computed,

$$\begin{aligned} \mathcal{C}_{1111} &= 66.51, & \mathcal{C}_{2112} &= 21.63, \\ \mathcal{C}_{1122} &= 20.06, & \mathcal{C}_{2121} &= 24.83, \\ \mathcal{C}_{1212} &= 24.83, & \mathcal{C}_{2211} &= 20.06, \\ \mathcal{C}_{1221} &= 21.63, & \mathcal{C}_{2222} &= 66.51, \end{aligned} \quad (85)$$

and terms not listed are zero. The equilibrium energy is -7.37563 eV/atom and nearest neighbor bond length 1.45 Å. For an assumed layer thickness of 3.4 Å, which is the standard layer separation thickness for

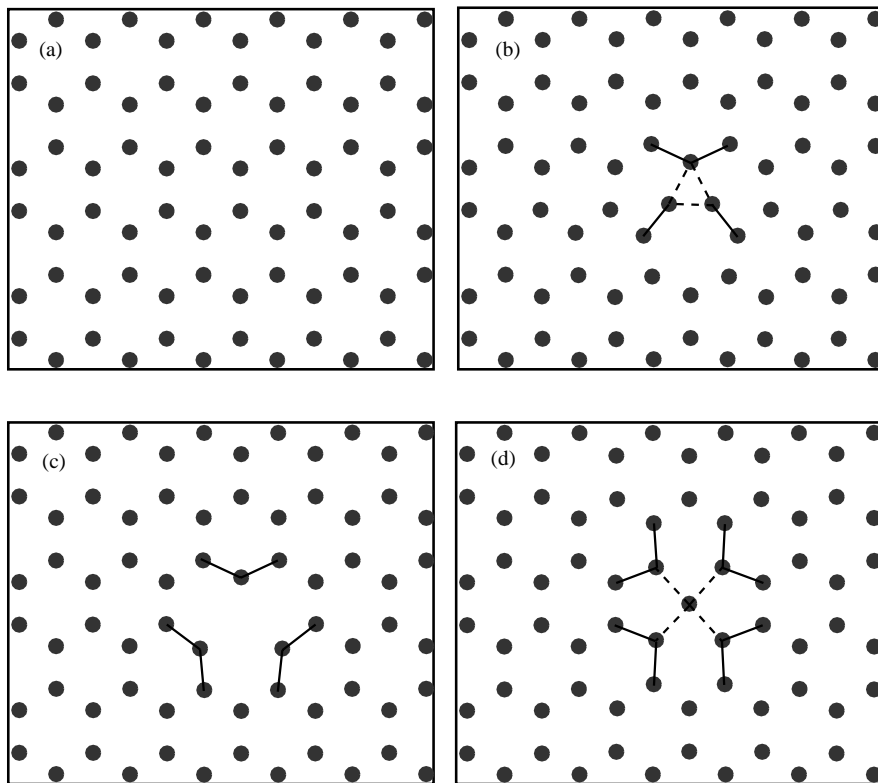


Fig. 6. Atom configurations in periodic cell. Lines are used to denote regions near the defect. (a) Defect-free, (b) interstitial, (c) equilibrium vacancy and (d) Saddle point vacancy.

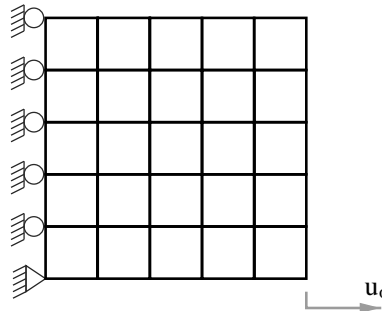


Fig. 7. Finite element model of macroscopic problem.

graphite, the effective Young's modulus from the bulk is $Y = 0.986$ TPa with an effective Poisson's ratio of 0.232. These values agree well with measured values for graphite and carbon nanotubes (Krishnan et al., 1998).

The model problem solved at the macroscopic scale is depicted in Fig. 7. The uniform grid is composed of 25 four-noded quadrilateral elements. The right edge is pulled uniformly and the left edge is held fixed. All units of measure are carried through in terms of eV and Å so that no assumption of a layer thickness is required. That is, although the problem is two-dimensional, there is no need for a plane assumption.

The solution procedure involves application of incremental loads with iterative loops over Eq. (47) and sub-loops over (43). The sub-loops seek converged values for $\mathbf{v}^{[1]}$ subject to the modification from Eq. (33). In this problem, an overly cautious load increment of 1.0×10^{-4} strain was used which ensured convergence tolerances for both $\mathbf{v}^{[0]}$ and $\mathbf{v}^{[1]}$ far beyond 10^{-8} Å.

The effective strain energy density and material properties are shown versus strain in Figs. 8 and 9. Of key interest are the sudden jumps that occur for the effective material properties of saddle point and interstitial defect scenarios at approximate strain values of 0.05 and 0.15, respectively. This is attributable to the relative instability of those types of point defects. Such observations were made previously for the saddle point vacancy in (Kaxiras and Pandey, 1988). The effective properties and energies at larger strains at and after the instability are meaningless and should not be used for inferences. The instability occurs in this problem because the separation distance between neighboring atoms near the point defect exceeds the cut-off radius because of the deformation, thereby distorting the strain energy and effective properties. We expect that the actual maximum allowable strain before instability occurs is much smaller because of the present zero-temperature assumption.

It is noteworthy that the approximate atom density in the longitudinal direction decreases (cell elongates) while it increases in the transverse direction. The subsequent material nonlinear affect it has on the properties is decrease in C_{1111} while increase in C_{2222} . We also note that the interstitial point defect possesses the highest values for material properties and lowest strain energy while the trends for the saddle point vacancy are precisely the reverse. The defect-free structure exhibits stronger material properties and higher strain energy than the equilibrium vacancy structure.

Comparing convergence rates between methodologies with homogenization (i.e., $\mathbf{v}^{[1]} \neq 0$) and without homogenization (i.e., $\mathbf{v}^{[1]} = 0$) shows the former with a distinct advantage.² The equilibrium vacancy configuration is used here. The convergence results are illustrated in Fig. 10. The calculation is of the transverse displacement of the upper right corner node of the mesh in Fig. 7 as it evolves with the total

² The methodology without homogenization implies an approach whose material property tensor is computed directly from the second derivative of the energy potential and whose formulation does not involve a perturbative term.

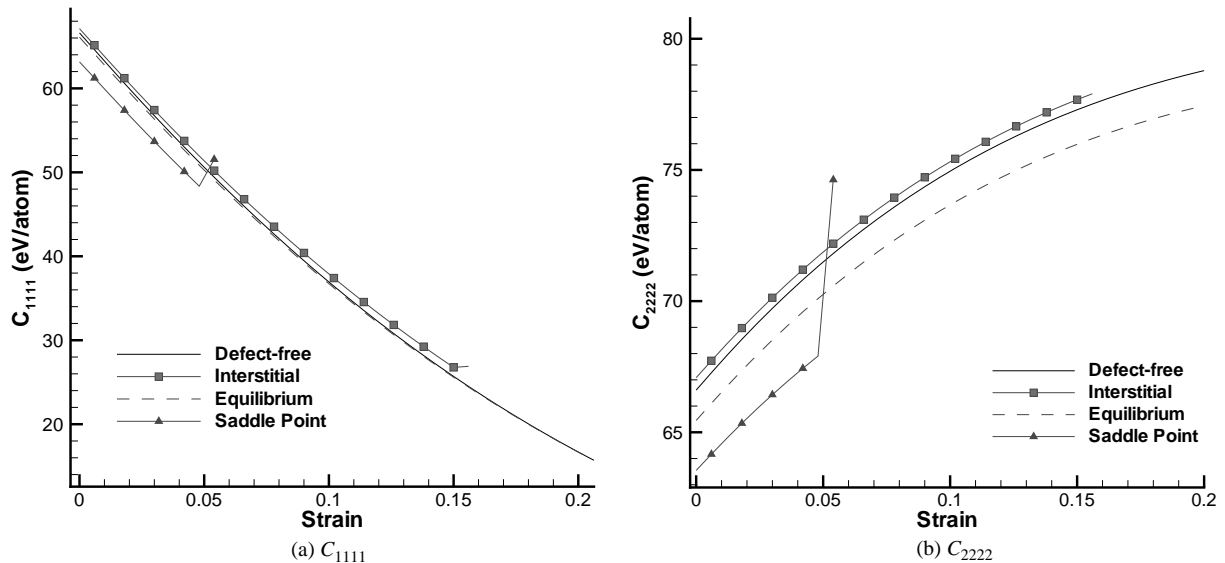


Fig. 8. Material property change with applied uniform strain.

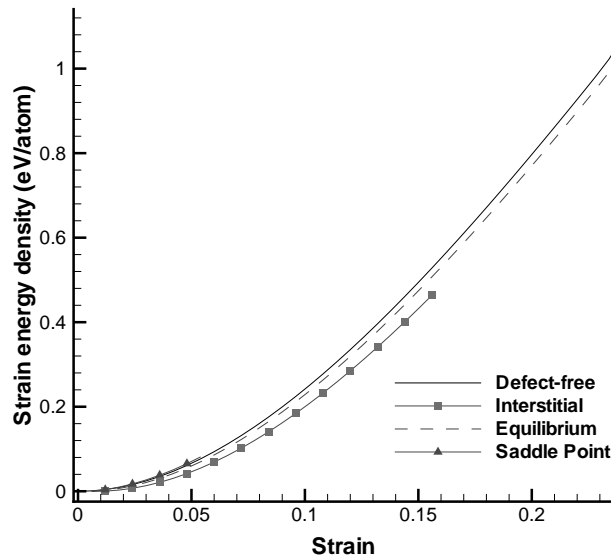


Fig. 9. Strain energy with applied uniform strain.

number of computation cycles, N_{steps} . The computation cycle is computed by adding the total number of nonlinear iterations steps (major loops plus sub-loops) with the total number of load increments, which is a crude way to estimate the convergence behavior. The number of load increments is selected to ensure that the final transverse displacement in the two methods is less than one percent different in magnitude. Fig. 10 shows that the total required number of calculation steps is smaller in the homogenization result by a factor of four.

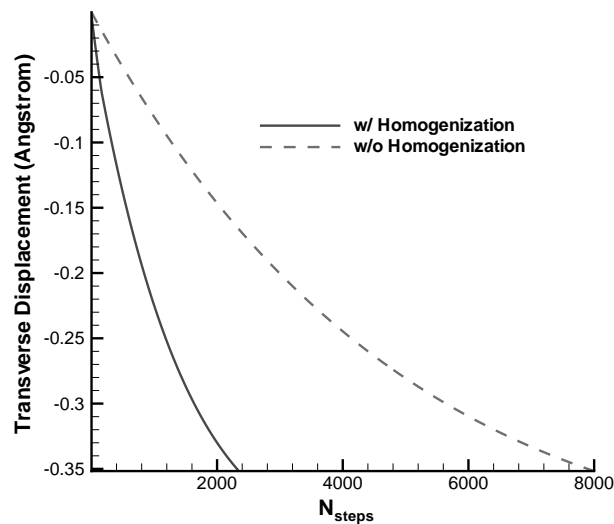


Fig. 10. Convergence with and without homogenization.

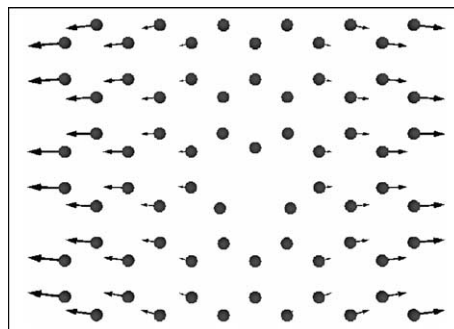


Fig. 11. Atom displacements due to global deformation.

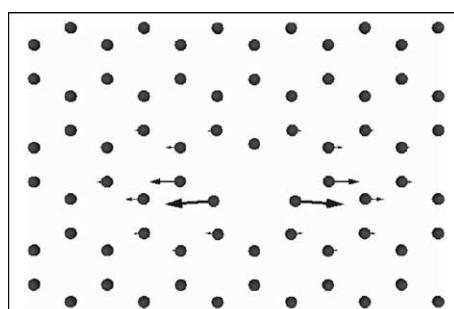


Fig. 12. Atom displacements due to homogenization method.

This convergence behavior is attributable to the addition of the $\mathbf{v}^{[1]}$ term in Eq. (33), which is closer to the energy minimizing configuration than Eq. (32) alone. Fig. 11 illustrates the atom displacement due to Eq. (32) relative to a local coordinate system centered on the periodic cell, and Fig. 12 illustrates the subsequent correction from Eq. (33). Arrow sizes correspond to relative magnitude of displacement.

The uniform strain applied in this example results in a uniform state of strain throughout the entire mesh in Fig. 7. It should be noted that more complex loading scenarios can be treated merely by changing the boundary conditions of the problem. These simple results, however, are indicative of the generality of the method for two and three dimensional problems.

8. Closing remarks

Linking atomic scale physics with continuum scale phenomena is of keen interest in the mechanical study of solids and nanostructures. The effects that dominate the mechanical behavior at the continuum scale typically initiate and evolve from the atomic scale. Moreover, periodic structures can emanate from nanopatterning and epitaxy through stresses induced from an underlying substrate. Despite numerous promising methods in the literature that are capable of linking scales up to the micron level, periodic structures with global dimensions at and beyond the millimeter range – needed for mass producing nanoscale devices – have only begun to be studied. To this end, we have attempted to exploit the features of homogenization theory to devise a scheme which passes atomistic information to very large continuum scales.

We have applied the Cauchy–Born rule to the atom scale by assuming that the configuration of atoms used to solve for the perturbation displacement at each load increment is indeed the minimizing configuration of the atomistic energy. We have not considered the method in conjunction with a lattice statics routine, i.e., various strategies of minimizing the atomistic energy by quenched molecular dynamics or solving Newton's equations to minimize the interatom forces. These assumptions (i.e., zero temperature and Cauchy–Born) also precludes the formulation from modeling thermally activated phenomena such as crack growth, propagation, or damage evolution. However, it can be used to estimate mechanical effects across coupled length scales and, if needed, serve as the underlying framework for modified algorithms that can account for such problems.

We demonstrated the method for one and two dimensional problems containing point defects. Mechanical data were reported from numerical experiments. The paucity of experimental data for nanomechanics makes validation difficult. However, the material properties stemming from the reference configuration compares very well with available published measurements and the observed trends from mechanical deformation agree with generally accepted intuition.

For this work, a form of the Tersoff–Brenner Type II potential was considered. But the principles and the general equations can be extended to any potential, provided the appropriate derivatives can be obtained as in Appendix A. Typically for classical systems, onerous tensor algebra and calculus are required or more computationally efficient procedures can be implemented to obtain derivatives numerically (Allen and Tildesley, 1987).

The aim of this paper was to develop an approach by which atomistic physics can be embedded into a continuum formulation for large scale systems. This goal has been achieved by formulating a consistent set of equations involving a classical atomistic potential at the fine scale and general finite strain and deformation elasticity at the coarse scale. Simple 1-D analytical results and 2-D numerical experiments were shown to illustrate the approach and its features. More realistic multiaxial problems in two and three dimensions for more detailed validation are the subjects of ongoing work.

Acknowledgements

Partial support by the US Army Research Laboratory Director's Research Initiative (DRI) Program under award number FY01-CIS-27 and the National Research Council Resident Research Associateship Program are gratefully acknowledged. A portion of this work was initiated while Dr. Peter W. Chung held a post-doctoral position at the University of Minnesota with Professor Kumar Tamma.

We gratefully acknowledge Mr. Brian Henz and Dr. Charles Cornwell for performing numerous quenched molecular dynamics runs and obtaining the reference configurations for the point defects. Also thanks to Mr. Jerry Clarke for providing substantial visualization assistance.

Appendix A. Derivatives of the Tersoff–Brenner Potential

The derivatives needed to form the Euler–Lagrange equations and the Hessian are shown here in detail. To simplify the notation, we define the following expressions,

$$r_{(ij)} = |\mathbf{r}_{(ij)}|, \quad (\text{A.1})$$

and

$$f'_{(ij)}(r) = \frac{\partial f_{(ij)}}{\partial r_{(ij)}} \quad f''_{(ij)}(r) = \frac{\partial^2 f_{(ij)}}{\partial r_{(ij)}^2}. \quad (\text{A.2})$$

Note that although the equations are written in component form with respect to atoms, it is still in dyadic notation due to the multiaxial components of $\mathbf{r}_{(ij)}$. That is, $r_{(ij)} \cdot \mathbf{e}_1$ is the component of the vector originating at atom i and terminating at atom j in the direction of \mathbf{e}_1 , $r_{(ij)} \cdot \mathbf{e}_2$ is the component in the direction of \mathbf{e}_2 , etc. From Eqs. (35)–(41), the derivatives in Eq. (49) are defined by

$$\frac{\partial E_b}{\partial \mathbf{r}_{(ij)}} = \sum_i \sum_{j(>i)} \left[V'_R \frac{\partial r_{(ij)}}{\partial \mathbf{r}_{(ij)}} - V_A \frac{\partial \bar{B}}{\partial \mathbf{r}_{(ij)}} - \bar{B} V'_A \frac{\partial r_{(ij)}}{\partial \mathbf{r}_{(ij)}} \right], \quad (\text{A.3})$$

$$\frac{\partial E_b}{\partial \mathbf{r}_{(ik)}} = \sum_i \sum_{j(>i)} \left[-V_A \frac{\partial \bar{B}}{\partial \mathbf{r}_{(ik)}} \right], \quad (\text{A.4})$$

$$\frac{\partial E_b}{\partial \mathbf{r}_{(jk)}} = \sum_i \sum_{j(>i)} \left[-V_A \frac{\partial \bar{B}}{\partial \mathbf{r}_{(jk)}} \right], \quad (\text{A.5})$$

$$\frac{\partial V_R}{\partial r_{(ij)}} = V'_R = f'_{(ij)} \frac{D^{(e)}}{(S-1)} e^{-\alpha_1(r_{(ij)}-R^{(e)})} - \alpha_1 \frac{f_{(ij)} D^{(e)}}{(S-1)} e^{-\alpha_1(r_{(ij)}-R^{(e)})}, \quad (\text{A.6})$$

$$\frac{\partial V_A}{\partial r_{(ij)}} = V'_A = f'_{(ij)} \frac{D^{(e)} S}{(S-1)} e^{-\alpha_2(r_{(ij)}-R^{(e)})} - \alpha_2 \frac{f_{(ij)} D^{(e)} S}{(S-1)} e^{-\alpha_2(r_{(ij)}-R^{(e)})}, \quad (\text{A.7})$$

$$\frac{\partial \bar{B}}{\partial \mathbf{r}_{(ij)}} = \frac{1}{2} \left\{ -\delta B_{(ij)}^{1+\frac{1}{\delta}} \sum_{k \neq (i,j)} \left[\frac{\partial G(\theta_{(ijk)})}{\partial \mathbf{r}_{(ij)}} f_{(ik)} \right] - \delta B_{(ji)}^{1+\frac{1}{\delta}} \sum_{k \neq (i,j)} \left[\frac{\partial G(\theta_{(jik)})}{\partial \mathbf{r}_{(ij)}} f_{(ik)} \right] \right\}, \quad (\text{A.8})$$

$$\frac{\partial \bar{B}}{\partial \mathbf{r}_{(ik)}} = -\frac{\delta}{2} B_{(ij)}^{1+\frac{1}{\delta}} \sum_{k \neq (i,j)} \left[\frac{\partial G(\theta_{(ijk)})}{\partial \mathbf{r}_{(ik)}} f_{(ik)} + G(\theta_{(ijk)}) f'_{(ik)} \frac{\partial r_{(ik)}}{\partial \mathbf{r}_{(ik)}} \right], \quad (\text{A.9})$$

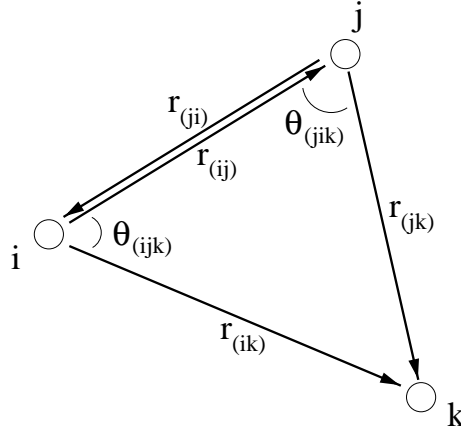


Fig. 13. Angles and interatom vectors.

$$\frac{\partial \bar{B}}{\partial \mathbf{r}_{(jk)}} = -\frac{\delta}{2} B_{(ji)}^{1+\delta} \sum_{k \neq (i,j)} \left[\frac{\partial G(\theta_{(jik)})}{\partial \mathbf{r}_{(jk)}} f_{jk} + G(\theta_{(jik)}) f'_{jk} \frac{\partial r_{(jk)}}{\partial \mathbf{r}_{(jk)}} \right], \quad (\text{A.10})$$

$$\frac{\partial G(\theta_\gamma)}{\partial \mathbf{r}_{(mn)}} = \frac{2a_0 c_0^2 (1 + \cos \theta_\gamma)}{[d_0^2 + (1 + \cos \theta_\gamma)^2]^2} \frac{\partial \cos \theta_\gamma}{\partial \mathbf{r}_{(mn)}}, \quad (\text{A.11})$$

for $(mn) = (ij)$ or (ik) when $\gamma = (ijk)$ and $(mn) = (ij)$ or (jk) when $\gamma = (jik)$. The angles $\theta_{(ijk)}$ and $\theta_{(jik)}$, shown in Fig. 13, are the angles subtending the connecting lines at the atoms i and j , respectively. Note that $\mathbf{r}_{(ij)} = -\mathbf{r}_{(ji)}$. The following identities can also be shown:

$$\begin{aligned} \frac{\partial r_{(ij)}}{\partial \mathbf{r}_{(ij)}} &= \frac{\partial (\mathbf{r}_{(ij)} \cdot \mathbf{r}_{(ij)})^{1/2}}{\partial \mathbf{r}_{(ij)}} \\ &= \frac{1}{2} \frac{1}{r_{(ij)}} 2\mathbf{r}_{(ij)} \\ &= \frac{\mathbf{r}_{(ij)}}{r_{(ij)}}, \end{aligned} \quad (\text{A.12})$$

$$\begin{aligned} \frac{\partial \cos \theta_{(ijk)}}{\partial \mathbf{r}_{(ij)}} &= \frac{\partial}{\partial \mathbf{r}_{(ij)}} \left(\frac{\mathbf{r}_{(ij)} \cdot \mathbf{r}_{(ik)}}{r_{(ij)} r_{(ik)}} \right) \\ &= \frac{\mathbf{r}_{(ik)}}{r_{(ij)} r_{(ik)}} - \frac{\mathbf{r}_{(ij)}}{r_{(ij)}^2} \cos \theta_{(ijk)}, \end{aligned} \quad (\text{A.13})$$

$$\frac{\partial \cos \theta_{(ijk)}}{\partial \mathbf{r}_{(ik)}} = \frac{\mathbf{r}_{(ij)}}{r_{(ij)} r_{(ik)}} - \frac{\mathbf{r}_{(ik)}}{r_{(ik)}^2} \cos \theta_{(ijk)}, \quad (\text{A.14})$$

$$\frac{\partial \cos \theta_{(jik)}}{\partial \mathbf{r}_{(ij)}} = -\frac{\mathbf{r}_{(jk)}}{r_{(ji)} r_{(jk)}} + \frac{\mathbf{r}_{(ji)}}{r_{(ji)}^2} \cos \theta_{(jik)}, \quad (\text{A.15})$$

$$\frac{\partial \cos \theta_{(jik)}}{\partial \mathbf{r}_{(jk)}} = \frac{\mathbf{r}_{(ji)}}{r_{(ji)} r_{(jk)}} - \frac{\mathbf{r}_{(jk)}}{r_{(jk)}^2} \cos \theta_{(jik)}. \quad (\text{A.16})$$

It is important to note that

$$\frac{\partial \mathbf{r}_{(ij)}}{\partial \mathbf{q}_{(m)}} = \begin{cases} -\mathbf{I} & m = i \\ \mathbf{I} & m = j \\ \mathbf{0} & m \neq (i, j) \end{cases}, \quad (\text{A.17})$$

where \mathbf{I} is the 3×3 identity tensor for a 3-D system. The derivative with respect to $\mathbf{r}_{(ik)}$ can be obtained likewise. This indicates that the summations in Eqs. (A.3), (A.4), (A.8) and (A.9), when multiplied by Eq. (A.17) in Eq. (49) are nontrivial if and only if m is equal to i , j , or k .

For the Hessian in Eq. (50), the differential terms are defined by

$$\begin{aligned} \frac{\partial^2 E_b}{\partial \mathbf{r}_{(ij)} \partial \mathbf{r}_{(ij)}} &= \sum_i \sum_{j(>i)} \left[\left(V''_R - \bar{B} V''_A \right) \left(\frac{\partial r_{(ij)}}{\partial \mathbf{r}_{(ij)}} \otimes \frac{\partial r_{(ij)}}{\partial \mathbf{r}_{(ij)}} \right) + V'_A \frac{\partial^2 r_{(ij)}}{\partial \mathbf{r}_{(ij)} \partial \mathbf{r}_{(ij)}} - V'_A \left(\frac{\partial \bar{B}}{\partial \mathbf{r}_{(ij)}} \otimes \frac{\partial r_{(ij)}}{\partial \mathbf{r}_{(ij)}} \right) \right. \\ &\quad \left. - V_A \frac{\partial^2 \bar{B}}{\partial \mathbf{r}_{(ij)} \partial \mathbf{r}_{(ij)}} - V'_A \left(\frac{\partial r_{(ij)}}{\partial \mathbf{r}_{(ij)}} \otimes \frac{\partial \bar{B}}{\partial \mathbf{r}_{(ij)}} \right) \right], \end{aligned} \quad (\text{A.18})$$

$$\frac{\partial^2 E_b}{\partial \mathbf{r}_{(ij)} \partial \mathbf{r}_{(ik)}} = \sum_i \sum_{j(>i)} \left[- V'_A \left(\frac{\partial \bar{B}}{\partial \mathbf{r}_{(ik)}} \otimes \frac{\partial r_{(ij)}}{\partial \mathbf{r}_{(ij)}} \right) - V_A \frac{\partial^2 \bar{B}}{\partial \mathbf{r}_{(ij)} \partial \mathbf{r}_{(ik)}} \right], \quad (\text{A.19})$$

$$\frac{\partial^2 E_b}{\partial \mathbf{r}_{(ik)} \partial \mathbf{r}_{(ij)}} = \sum_i \sum_{j(>i)} \left[- V'_A \left(\frac{\partial r_{(ij)}}{\partial \mathbf{r}_{(ij)}} \otimes \frac{\partial \bar{B}}{\partial \mathbf{r}_{(ik)}} \right) - V_A \frac{\partial^2 \bar{B}}{\partial \mathbf{r}_{(ik)} \partial \mathbf{r}_{(ij)}} \right], \quad (\text{A.20})$$

$$\frac{\partial^2 E_b}{\partial \mathbf{r}_{(ik)} \partial \mathbf{r}_{(ik)}} = \sum_i \sum_{j(>i)} \left[- V_A \frac{\partial^2 \bar{B}}{\partial \mathbf{r}_{(ik)} \partial \mathbf{r}_{(ik)}} \right], \quad (\text{A.21})$$

$$\frac{\partial^2 E_b}{\partial \mathbf{r}_{(jk)} \partial \mathbf{r}_{(jk)}} = \sum_i \sum_{j(>i)} \left[- V_A \frac{\partial^2 \bar{B}}{\partial \mathbf{r}_{(jk)} \partial \mathbf{r}_{(jk)}} \right], \quad (\text{A.22})$$

$$\frac{\partial^2 E_b}{\partial \mathbf{r}_{(ij)} \partial \mathbf{r}_{(jk)}} = \sum_i \sum_{j(>i)} \left[- V'_A \left(\frac{\partial r_{(ij)}}{\partial \mathbf{r}_{(ij)}} \otimes \frac{\partial \bar{B}}{\partial \mathbf{r}_{(jk)}} \right) - V_A \frac{\partial^2 \bar{B}}{\partial \mathbf{r}_{(ij)} \partial \mathbf{r}_{(jk)}} \right], \quad (\text{A.23})$$

$$\frac{\partial^2 E_b}{\partial \mathbf{r}_{(jk)} \partial \mathbf{r}_{(ij)}} = \sum_i \sum_{j(>i)} \left[- V'_A \left(\frac{\partial \bar{B}}{\partial \mathbf{r}_{(jk)}} \otimes \frac{\partial r_{(ij)}}{\partial \mathbf{r}_{(ij)}} \right) - V_A \frac{\partial^2 \bar{B}}{\partial \mathbf{r}_{(jk)} \partial \mathbf{r}_{(ij)}} \right], \quad (\text{A.24})$$

$$\frac{\partial^2 E_b}{\partial \mathbf{r}_{(ik)} \partial \mathbf{r}_{(jk)}} = \sum_i \sum_{j(>i)} \left[- V_A \frac{\partial^2 \bar{B}}{\partial \mathbf{r}_{(ik)} \partial \mathbf{r}_{(jk)}} \right], \quad (\text{A.25})$$

$$\frac{\partial^2 E_b}{\partial \mathbf{r}_{(jk)} \partial \mathbf{r}_{(ik)}} = \sum_i \sum_{j(>i)} \left[- V_A \frac{\partial^2 \bar{B}}{\partial \mathbf{r}_{(jk)} \partial \mathbf{r}_{(ik)}} \right], \quad (\text{A.26})$$

and additional algebra yields

$$V_R'' = \frac{\partial^2 V_R}{\partial r_{(ij)} \partial r_{(ij)}} = \left[\frac{f_{(ij)}'' D^{(e)}}{(S-1)} - \frac{2\alpha_1 f_{(ij)}' D^{(e)}}{(S-1)} + \frac{\alpha_1^2 f_{(ij)} D^{(e)}}{(S-1)} \right] e^{-\alpha_1(r_{(ij)} - R^{(e)})}, \quad (\text{A.27})$$

$$V_A'' = \frac{\partial^2 V_A}{\partial r_{(ij)} \partial r_{(ij)}} = \left[\frac{f_{(ij)}'' D^{(e)} S}{(S-1)} - \frac{2\alpha_2 f_{(ij)}' D^{(e)} S}{(S-1)} + \frac{\alpha_2^2 f_{(ij)} D^{(e)} S}{(S-1)} \right] e^{-\alpha_2(r_{(ij)} - R^{(e)})}, \quad (\text{A.28})$$

$$\begin{aligned} \frac{\partial^2 \bar{B}}{\partial \mathbf{r}_{(ij)} \partial \mathbf{r}_{(ij)}} &= -\frac{(\delta+1)}{2} B_{(ij)}^{\frac{1}{\delta}} \sum_{k \neq (i,j)} f_{(ik)} \left(\frac{\partial G(\theta_{(ijk)})}{\partial \mathbf{r}_{(ij)}} \otimes \frac{\partial B_{(ij)}}{\partial \mathbf{r}_{(ij)}} \right) - \frac{\delta}{2} B_{(ij)}^{1+\frac{1}{\delta}} \sum_{k \neq (i,j)} \left(f_{(ik)} \frac{\partial^2 G(\theta_{(ijk)})}{\partial \mathbf{r}_{(ij)} \partial \mathbf{r}_{(ij)}} \right), \\ &\quad -\frac{(\delta+1)}{2} B_{(ji)}^{\frac{1}{\delta}} \sum_{k \neq (i,j)} f_{jk} \left(\frac{\partial G(\theta_{(jik)})}{\partial \mathbf{r}_{(ij)}} \otimes \frac{\partial B_{(ji)}}{\partial \mathbf{r}_{(ij)}} \right) - \frac{\delta}{2} B_{(ji)}^{1+\frac{1}{\delta}} \sum_{k \neq (i,j)} \left(f_{jk} \frac{\partial^2 G(\theta_{(jik)})}{\partial \mathbf{r}_{(ij)} \partial \mathbf{r}_{(ij)}} \right), \end{aligned} \quad (\text{A.29})$$

$$\begin{aligned} \frac{\partial^2 \bar{B}}{\partial \mathbf{r}_{(ij)} \partial \mathbf{r}_{(ik)}} &= -\frac{(\delta+1)}{2} B_{(ij)}^{\frac{1}{\delta}} \sum_{k \neq (i,j)} \left[f_{(ik)} \left(\frac{\partial G(\theta_{(ijk)})}{\partial \mathbf{r}_{(ik)}} \otimes \frac{\partial B_{(ij)}}{\partial \mathbf{r}_{(ij)}} \right) + G(\theta_{(ijk)}) f_{(ik)}' \left(\frac{\partial r_{(ik)}}{\partial \mathbf{r}_{(ik)}} \otimes \frac{\partial B_{(ij)}}{\partial \mathbf{r}_{(ij)}} \right) \right] \\ &\quad -\frac{\delta}{2} B_{(ij)}^{1+\frac{1}{\delta}} \sum_{k \neq (i,j)} \left[f_{(ik)} \frac{\partial^2 G(\theta_{(ijk)})}{\partial \mathbf{r}_{(ij)} \partial \mathbf{r}_{(ik)}} + f_{(ik)}' \left(\frac{\partial G(\theta_{(ijk)})}{\partial \mathbf{r}_{(ik)}} \otimes \frac{\partial G(\theta_{(ijk)})}{\partial \mathbf{r}_{(ij)}} \right) \right], \end{aligned} \quad (\text{A.30})$$

$$\begin{aligned} \frac{\partial^2 \bar{B}}{\partial \mathbf{r}_{(ik)} \partial \mathbf{r}_{(ij)}} &= -\frac{(\delta+1)}{2} B_{(ij)}^{\frac{1}{\delta}} \sum_{k \neq (i,j)} \left[f_{(ik)} \left(\frac{\partial G(\theta_{(ijk)})}{\partial \mathbf{r}_{(ij)}} \otimes \frac{\partial B_{(ij)}}{\partial \mathbf{r}_{(ik)}} \right) \right] \\ &\quad -\frac{\delta}{2} B_{(ij)}^{1+\frac{1}{\delta}} \sum_{k \neq (i,j)} \left[f_{(ik)} \frac{\partial^2 G(\theta_{(ijk)})}{\partial \mathbf{r}_{(ik)} \partial \mathbf{r}_{(ij)}} + f_{(ik)}' \left(\frac{\partial G(\theta_{(ijk)})}{\partial \mathbf{r}_{(ij)}} \otimes \frac{\partial r_{(ik)}}{\partial \mathbf{r}_{(ik)}} \right) \right], \end{aligned} \quad (\text{A.31})$$

$$\begin{aligned} \frac{\partial^2 \bar{B}}{\partial \mathbf{r}_{(ik)} \partial \mathbf{r}_{(ik)}} &= -\frac{(\delta+1)}{2} B_{(ij)}^{\frac{1}{\delta}} \sum_{k \neq (i,j)} \left[f_{(ik)} \left(\frac{\partial G(\theta_{(ijk)})}{\partial \mathbf{r}_{(ik)}} \otimes \frac{\partial B_{(ij)}}{\partial \mathbf{r}_{(ik)}} \right) + G(\theta_{(ijk)}) f_{(ik)}' \left(\frac{\partial r_{(ik)}}{\partial \mathbf{r}_{(ik)}} \otimes \frac{\partial B_{(ij)}}{\partial \mathbf{r}_{(ik)}} \right) \right] \\ &\quad -\frac{\delta}{2} B_{(ij)}^{1+\frac{1}{\delta}} \sum_{k \neq (i,j)} \left[f_{(ik)} \frac{\partial^2 G(\theta_{(ijk)})}{\partial \mathbf{r}_{(ik)} \partial \mathbf{r}_{(ik)}} + 2f_{(ik)}' \left(\frac{\partial r_{(ik)}}{\partial \mathbf{r}_{(ik)}} \otimes \frac{\partial G(\theta_{(ijk)})}{\partial \mathbf{r}_{(ik)}} \right) + G(\theta_{(ijk)}) f_{(ik)}'' \left(\frac{\partial r_{(ik)}}{\partial \mathbf{r}_{(ik)}} \otimes \frac{\partial r_{(ik)}}{\partial \mathbf{r}_{(ik)}} \right) \right. \\ &\quad \left. + G(\theta_{(ijk)}) f_{(ik)}' \frac{\partial^2 r_{(ik)}}{\partial \mathbf{r}_{(ik)} \partial \mathbf{r}_{(ik)}} \right], \end{aligned} \quad (\text{A.32})$$

$$\begin{aligned} \frac{\partial^2 \bar{B}}{\partial \mathbf{r}_{(ij)} \partial \mathbf{r}_{(jk)}} &= -\frac{(\delta+1)}{2} B_{(ji)}^{\frac{1}{\delta}} \sum_{k \neq (i,j)} \left[f_{jk} \left(\frac{\partial G(\theta_{(jik)})}{\partial \mathbf{r}_{(jk)}} \otimes \frac{\partial B_{(ji)}}{\partial \mathbf{r}_{(ij)}} \right) + G(\theta_{(jik)}) f_{jk}' \left(\frac{\partial r_{(jk)}}{\partial \mathbf{r}_{(jk)}} \otimes \frac{\partial B_{(ji)}}{\partial \mathbf{r}_{(ij)}} \right) \right] \\ &\quad -\frac{\delta}{2} B_{(ji)}^{1+\frac{1}{\delta}} \sum_{k \neq (i,j)} \left[f_{jk} \frac{\partial^2 G(\theta_{(jik)})}{\partial \mathbf{r}_{(ij)} \partial \mathbf{r}_{(jk)}} + f_{jk}' \left(\frac{\partial G(\theta_{(jik)})}{\partial \mathbf{r}_{(jk)}} \otimes \frac{\partial G(\theta_{(jik)})}{\partial \mathbf{r}_{(ij)}} \right) \right], \end{aligned} \quad (\text{A.33})$$

$$\begin{aligned} \frac{\partial^2 \bar{B}}{\partial \mathbf{r}_{(jk)} \partial \mathbf{r}_{(ij)}} &= -\frac{(\delta+1)}{2} B_{(ji)}^{\frac{1}{\delta}} \sum_{k \neq (i,j)} \left[f_{jk} \left(\frac{\partial G(\theta_{(jik)})}{\partial \mathbf{r}_{(ij)}} \otimes \frac{\partial B_{(ji)}}{\partial \mathbf{r}_{(jk)}} \right) \right] \\ &\quad -\frac{\delta}{2} B_{(ji)}^{1+\frac{1}{\delta}} \sum_{k \neq (i,j)} \left[f_{jk} \frac{\partial^2 G(\theta_{(jik)})}{\partial \mathbf{r}_{(jk)} \partial \mathbf{r}_{(ij)}} + f_{jk}' \left(\frac{\partial G(\theta_{(jik)})}{\partial \mathbf{r}_{(ij)}} \otimes \frac{\partial r_{(jk)}}{\partial \mathbf{r}_{(jk)}} \right) \right], \end{aligned} \quad (\text{A.34})$$

$$\begin{aligned} \frac{\partial^2 \bar{B}}{\partial \mathbf{r}_{(jk)} \partial \mathbf{r}_{(jk)}} &= -\frac{(\delta+1)}{2} B_{(ji)}^4 \sum_{k \neq (i,j)} \left[f_{jk} \left(\frac{\partial G(\theta_{(jik)})}{\partial \mathbf{r}_{(jk)}} \otimes \frac{\partial B_{(ji)}}{\partial \mathbf{r}_{(jk)}} \right) + G(\theta_{(jik)}) f'_{jk} \left(\frac{\partial r_{(jk)}}{\partial \mathbf{r}_{(jk)}} \otimes \frac{\partial B_{(ji)}}{\partial \mathbf{r}_{(jk)}} \right) \right] \\ &\quad - \frac{\delta}{2} B_{(ji)}^{1+\frac{1}{\delta}} \sum_{k \neq (i,j)} \left[f_{jk} \frac{\partial^2 G(\theta_{(jik)})}{\partial \mathbf{r}_{(jk)} \partial \mathbf{r}_{(jk)}} + 2f'_{jk} \left(\frac{\partial r_{(jk)}}{\partial \mathbf{r}_{(jk)}} \otimes \frac{\partial G(\theta_{(jik)})}{\partial \mathbf{r}_{(jk)}} \right) + G(\theta_{(jik)}) f''_{jk} \left(\frac{\partial r_{(jk)}}{\partial \mathbf{r}_{(jk)}} \otimes \frac{\partial r_{(jk)}}{\partial \mathbf{r}_{(jk)}} \right) \right. \\ &\quad \left. + G(\theta_{(jik)}) f'_{jk} \frac{\partial^2 r_{(jk)}}{\partial \mathbf{r}_{(jk)} \partial \mathbf{r}_{(jk)}} \right], \end{aligned} \quad (\text{A.35})$$

$$\frac{\partial^2 \bar{B}}{\partial \mathbf{r}_{(ik)} \partial \mathbf{r}_{(jk)}} = \frac{\partial^2 \bar{B}}{\partial \mathbf{r}_{(jk)} \partial \mathbf{r}_{(ik)}} = \mathbf{0}, \quad (\text{A.36})$$

$$\frac{\partial^2 r_{(ij)}}{\partial \mathbf{r}_{(ij)} \partial \mathbf{r}_{(ij)}} = \frac{\mathbf{I}}{r_{(ij)}} - \frac{\mathbf{r}_{(ij)} \otimes \mathbf{r}_{(ij)}}{r_{(ij)}^3}. \quad (\text{A.37})$$

To complete the derivation, the following identities are needed:

$$\begin{aligned} \frac{\partial^2 G}{\partial \mathbf{r}_{(mn)} \partial \mathbf{r}_{(pq)}} &= \left(\frac{-8a_0 c_0^2 (1 + \cos \theta_\gamma)^2}{(d_0^2 + (1 + \cos \theta_\gamma)^2)^3} + \frac{2a_0 c_0^2}{(d_0^2 + (1 + \cos \theta_\gamma)^2)^2} \right) \left(\frac{\partial \cos \theta_\gamma}{\partial \mathbf{r}_{(pq)}} \otimes \frac{\partial \cos \theta_\gamma}{\partial \mathbf{r}_{(mn)}} \right) \\ &\quad + \frac{2a_0 c_0^2 (1 + \cos \theta_\gamma)}{(d_0^2 + (1 + \cos \theta_\gamma)^2)^2} \frac{\partial^2 \cos \theta_\gamma}{\partial \mathbf{r}_{(mn)} \partial \mathbf{r}_{(pq)}}, \end{aligned} \quad (\text{A.38})$$

with the appropriate combinations of $(mn, pq) = (ij, ij), (ij, ik), (ik, ij)$, and (ik, ik) for $\gamma = ijk$ and $(mn, pq) = (ij, jk), (jk, ij), (jk, jk)$ for $\gamma = jik$, and,

$$\frac{\partial^2 \cos \theta_{(ijk)}}{\partial \mathbf{r}_{(ij)} \partial \mathbf{r}_{(ij)}} = -\frac{1}{r_{(ij)}^3 r_{(ik)}} (\mathbf{r}_{(ij)} \otimes \mathbf{r}_{(ik)}) - \frac{\cos \theta_{(ijk)} \mathbf{I}}{r_{(ij)}^2} + \frac{3 \cos \theta_{(ijk)}}{r_{(ij)}^4} (\mathbf{r}_{(ij)} \otimes \mathbf{r}_{(ij)}) - \frac{1}{r_{(ij)}^3 r_{(ik)}} (\mathbf{r}_{(ik)} \otimes \mathbf{r}_{(ij)}), \quad (\text{A.39})$$

$$\frac{\partial^2 \cos \theta_{(ijk)}}{\partial \mathbf{r}_{(ij)} \partial \mathbf{r}_{(ik)}} = -\frac{1}{r_{(ij)}^3 r_{(ik)}} (\mathbf{r}_{(ij)} \otimes \mathbf{r}_{(ij)}) - \frac{1}{r_{(ij)} r_{(ik)}^3} (\mathbf{r}_{(ik)} \otimes \mathbf{r}_{(ik)}) + \frac{\cos \theta_{(ijk)}}{r_{(ij)}^2 r_{(ik)}^2} (\mathbf{r}_{(ik)} \otimes \mathbf{r}_{(ij)}) + \frac{\mathbf{I}}{r_{(ij)} r_{(ik)}}, \quad (\text{A.40})$$

$$\frac{\partial^2 \cos \theta_{(ijk)}}{\partial \mathbf{r}_{(ik)} \partial \mathbf{r}_{(ij)}} = -\frac{1}{r_{(ij)}^3 r_{(ik)}} (\mathbf{r}_{(ij)} \otimes \mathbf{r}_{(ij)}) - \frac{1}{r_{(ij)} r_{(ik)}^3} (\mathbf{r}_{(ik)} \otimes \mathbf{r}_{(ik)}) + \frac{\cos \theta_{(ijk)}}{r_{(ij)}^2 r_{(ik)}^2} (\mathbf{r}_{(ij)} \otimes \mathbf{r}_{(ik)}) + \frac{\mathbf{I}}{r_{(ij)} r_{(ik)}}, \quad (\text{A.41})$$

$$\frac{\partial^2 \cos \theta_{(ijk)}}{\partial \mathbf{r}_{(ik)} \partial \mathbf{r}_{(ik)}} = -\frac{1}{r_{(ij)}^3 r_{(ik)}^3} (\mathbf{r}_{(ik)} \otimes \mathbf{r}_{(ij)}) - \frac{\cos \theta_{(ijk)} \mathbf{I}}{r_{(ik)}^2} + \frac{3 \cos \theta_{(ijk)}}{r_{(ik)}^4} (\mathbf{r}_{(ik)} \otimes \mathbf{r}_{(ik)}) - \frac{1}{r_{(ij)} r_{(ik)}^3} (\mathbf{r}_{(ij)} \otimes \mathbf{r}_{(ik)}), \quad (\text{A.42})$$

$$\frac{\partial^2 \cos \theta_{(jik)}}{\partial \mathbf{r}_{(ji)} \partial \mathbf{r}_{(ji)}} = -\frac{1}{r_{(ji)}^3 r_{(jk)}} (\mathbf{r}_{(jk)} \otimes \mathbf{r}_{(ji)}) + \frac{\cos \theta_{(jik)} \mathbf{I}}{r_{(ji)}^2} + \frac{3 \cos \theta_{(jik)}}{r_{(ji)}^4} (\mathbf{r}_{(ji)} \otimes \mathbf{r}_{(ji)}) - \frac{1}{r_{(ji)}^3 r_{(jk)}} (\mathbf{r}_{(ji)} \otimes \mathbf{r}_{(jk)}), \quad (\text{A.43})$$

$$\frac{\partial^2 \cos \theta_{(jik)}}{\partial \mathbf{r}_{(ji)} \partial \mathbf{r}_{(jk)}} = \frac{1}{r_{(ji)}^3 r_{(jk)}} (\mathbf{r}_{(ji)} \otimes \mathbf{r}_{(ji)}) + \frac{1}{r_{(ji)} r_{(jk)}^3} (\mathbf{r}_{(jk)} \otimes \mathbf{r}_{(jk)}) - \frac{\cos \theta_{(jik)}}{r_{(ji)}^2 r_{(jk)}^2} (\mathbf{r}_{(jk)} \otimes \mathbf{r}_{(ji)}) - \frac{\mathbf{I}}{r_{(ji)} r_{(jk)}}, \quad (\text{A.44})$$

$$\frac{\partial^2 \cos \theta_{(jik)}}{\partial \mathbf{r}_{(jk)} \partial \mathbf{r}_{(ji)}} = \frac{1}{r_{(ji)}^3 r_{(jk)}} (\mathbf{r}_{(ji)} \otimes \mathbf{r}_{(ji)}) + \frac{1}{r_{(ji)} r_{(jk)}^3} (\mathbf{r}_{(jk)} \otimes \mathbf{r}_{(jk)}) - \frac{\cos \theta_{(jik)}}{r_{(ji)}^2 r_{(jk)}^2} (\mathbf{r}_{(ji)} \otimes \mathbf{r}_{(jk)}) - \frac{\mathbf{I}}{r_{(ji)} r_{(jk)}}, \quad (\text{A.45})$$

$$\frac{\partial^2 \cos \theta_{(jik)}}{\partial \mathbf{r}_{(jk)} \partial \mathbf{r}_{(jk)}} = -\frac{1}{r_{(ji)} r_{(jk)}^3} (\mathbf{r}_{(ji)} \otimes \mathbf{r}_{(jk)}) - \frac{\cos \theta_{(jik)} \mathbf{I}}{r_{(jk)}^2} + \frac{3 \cos \theta_{(jik)}}{r_{(jk)}^4} (\mathbf{r}_{(jk)} \otimes \mathbf{r}_{(jk)}) - \frac{1}{r_{(ji)} r_{(jk)}^3} (\mathbf{r}_{(jk)} \otimes \mathbf{r}_{(ji)}). \quad (\text{A.46})$$

This completes the closed-form derivation of the Hessian for the Tersoff–Brenner potential.

Despite the relative algebraic complexity of the expressions, the calculations can be performed readily using computers. The algorithm is based on an additive assembly process by casting the equations in their equivalent matrix forms and then summing over all unique pairs and triples of atoms, which translates well to an iterative computational methodology.

References

Allen, M.P., Tildesley, D.J., 1987. Computer Simulation of Liquids. Clarendon Press, Oxford.

Bakhvalov, N., Panasenko, G., 1989. Homogenization: Averaging Processes in Periodic Media. Kluwer.

Bensoussan, A., Lions, J.L., Papanicolaou, G., 1978. Asymptotic Analysis for Periodic Structures. North-Holland.

Brenner, D.W., 1990. Empirical potential for hydrocarbons for use in simulating the chemical vapor deposition of diamond films. *Physical Review B* 42 (15), 9458–9471.

Broughton, J.Q., Abraham, F.F., Bernstein, N., Kaxiras, E., 1999. Concurrent coupling of length scales: methodology and application. *Physical Review B* 60 (4), 2391–2403.

Cleri, F., Phillpot, S.R., Wolf, D., Yip, S., 1998. Atomistic simulations of materials fracture and the link between atomic and continuum length scales. *Journal of the American Ceramic Society* 81, 501–516.

Erickson, J.L., 1984. Phase Transformations and Material Instabilities in Solids. Academic Press Inc., pp. 61–77.

Hjort, M., Stafström, S., 2000. Modeling vacancies in graphite via the Hückel method. *Physical Review B* 61 (20), 14089–14094.

Kaxiras, E., Pandey, K.C., 1988. Energetics of defects and diffusion mechanisms in graphite. *Physical Review Letters* 61 (23), 2693–2696.

Krasheninnikov, A.V., Nordlund, K., Keinonen, J., 2002. Production of defects in supported carbon nanotubes under ion irradiation. *Physical Review B* 65, 165423–165431.

Krishnan, A., Dujardin, E., Ebbesen, T.W., Yianilos, P.N., Treacy, M.M.J., 1998. Young's modulus of single-walled nanotubes. *Physical Review B* 58 (20), 14013–14019.

Marsden, J.E., Hughes, T.J.R., 1983. Mathematical Foundations of Elasticity. Dover Publications Inc., New York.

Mullins, M., Dokainish, M.A., 1982. Simulation of the (001) plane crack in α -iron employing a new boundary scheme. *Philosophical Magazine A* 46, 771–787.

Mura, T., 1987. Micromechanics of Defects in Solids. Martinus Nijhoff Publishers, Dordrecht, the Netherlands.

Rosa, C.D., Park, C., Thomas, E.L., Lotz, B., 2000. Microdomain patterns from directional eutectic solidification and epitaxy. *Nature* 405, 433–437.

Rudd, R.E., Broughton, J.Q., 2000. Concurrent coupling of length scales in solid state systems. *Physica Status Solidi B-Basic Research* 217 (1), 251–291.

Sanchez-Palencia, E., 1980. Non-homogeneous Media and Vibration Theory: Lecture Notes in Physics, vol. 127. Springer-Verlag.

Sinclair, J., 1971. Improved atomistic model of a bcc dislocation core. *Journal of Applied Physics* 42, 5321–5329.

Tadmor, E.B., Ortiz, M., Phillips, R., 1996. Quasicontinuum analysis of defects in solids. *Philosophical Magazine A* 73 (6), 1529–1563.

Takano, N., Ohnishi, Y., Zako, M., Nishiyabu, K., 2000. The formulation of homogenization method applied to large deformation problem for composite materials. *International Journal of Solids and Structures* 37, 6517–6535.

Tang, Y.S., Torres, C.M.S., 1996. Damage, strain and quantum confinement issues in dry etched semiconductor nanostructures. In: Materials Research Society Symposium Proceedings, Surface/Interface and Stress Effects in Electronic Material Nanostructures, vol. 405. Materials Research Society, Pittsburgh, PA, USA, pp. 99–108.

Tersoff, J., 1988. Empirical interatomic potential for carbon, with applications to amorphous carbon. *Physical Review Letters* 61 (25), 2879–2882.